Tectonic evolution of Paleoproterozoic rocks in the Grand Canyon: Insights into middle-crustal processes

Bradley R. Ilg
Karl E. Karlstrom
Department of Earth and Planetary Sciences, University of New Mexico, Albuquerque, New Mexico 87131

David P. Hawkins
Department of Earth, Atmospheric, and Planetary Sciences, Massachusetts Institute of Technology, Cambridge, Massachusetts 02139

Michael L. Williams
Department of Geology and Geography, University of Massachusetts, Amherst, Massachusetts 01003

ABSTRACT

Paleoproterozoic supracrustal rocks of the Upper Granite Gorge are divided into three mappable units: the Rama, Brahma, and Vishnu Schists, here collectively named the "Granite Gorge Metamorphic Suite." The Brahma Schist consists of mafic to intermediate-composition metavolcanic rocks that have yielded an age of 1750 Ma. The Rama Schist consists of felsic metavolcanic rocks that have yielded an age of 1742 Ma. On the basis of the presence of relict pillow structures, interlayering of metavolcanic units, and the large volumes of metavolcanic rocks, the combined volcanic package is interpreted to be metamorphosed, island-arc–related, submarine volcanic rocks. The metavolcanic units are locally overlain by the metamorphosed, arc-basin, submarine sedimentary rocks of the Vishnu Schist.

The term "Zoroaster Plutonic Complex," previously used for all Paleoproterozoic and Mesoproterozoic plutonic rocks in the Grand Canyon, is abandoned in favor of use of names for individual plutons. Plutons are classified into two genetically and temporally separate intrusive suites: (1) 1740–1713 Ma plutons that are typically concordant to foliation, range in composition from gabbro to granodiorite, have calc-alkalic chemistry, and are interpreted to be arc-related plutons and (2) 1698–1662 Ma granite plutons, stocks, and pegmatite and aplite dikes that have textures and intrusive geometries indicating they were emplaced synchronously with peak metamorphism and northwest-southeast shortening.

The dominant tectonic fabric is a northeast-striking, subvertical, variably developed foliation (S_2) that is axial planar to plunging, open to isoclinal, upright, asymmetric folds (F_2) of an early, penetrative, apparently initially northwest-striking foliation (S_1). F_2 folds have wavelengths of kilometres and cause repetition of rock units across the transect. Partitioning of deformation in space and perhaps in time was strongly influenced by crustal heterogeneity. For example, plutons, pegmatite networks, and fold-hinge zones acted as buttresses, and S_2 high-strain domains and shear zones are localized at the margins of these features. Generally northeast-striking, S_2-related shear zones segment the transect into blocks. Shear zones last moved late during shortening and postdate the metamorphic peak. One of these, the Crystal shear zone, may be a fundamental crustal province boundary.

Paleoproterozoic rocks in the Grand Canyon record the accretion of 1750–1713 Ma island-arc rocks and their assembly to Laurentia via dynamic interaction of deformation, metamorphism, and magmatism over ≈20 m.y. Changes in styles of deformation from F_1-related thrusting and penetrative S_1 fabric development to F_2-related upright folding and variable S_2 fabric development coincided with changes in styles of magmatism. The 1740–1730 Ma arc-related mafic to intermediate-composition plutons preserve strong S_1 foliation. The 1717–1713 Ma arc-related plutons preserve weak S_1 tectonic layering and locally strong S_2 strain. The 1698–1685 Ma granitic plutonism locally preceded S_2 and F_2 strain and was regionally synchronous with peak S_2 and F_2 strain (1700–1685 Ma) and peak metamorphism (1706–1697 Ma). More limited deformation and plutonism continued until at least 1662 Ma.

INTRODUCTION

Paleoproterozoic rocks of the southwestern United States record the growth of the Laurentian supercontinent by addition of dominantly juvenile crust from 1.8 to 1.6 Ga (Karlstrom and Bowring, 1988; Hoffman, 1988). Rocks exposed across this orogenic belt offer important insights into the processes of accretion of juvenile continental crust, processes associated with convergent assembly of arcs at middle-crustal levels, and the history of stabilization of continental lithosphere (Bowring and Karlstrom, 1990). Work to date in the American Southwest continues to emphasize a complex polyphase history of Proterozoic tectonism, such that (1) the nature and location of possible early accretionary boundaries (or sutures) remain enigmatic (e.g., Bergh and Karlstrom, 1992; Karlstrom and Bowring, 1993), (2) interpretation of terranes and provinces is controversial (Karlstrom and Daniel, 1993; Wooden and DeWitt, 1991; Bennett and DePaolo, 1987; Van Schmus et al., 1993), and (3) thermal, baric, and deformational histories of different parts of the orogen record different parts of a 200-m.y.-long progressive tectonic history.

This paper presents a synthesis of the tectonic history of Paleoproterozoic rocks of the Upper Granite Gorge of the Grand Canyon. This area provides one of the few windows through the Paleozoic rocks of the Colorado Plateau and thus is important for comparing basement transects in the Arizona Transition Zone to those of the Rocky Mountain region. The transect is ≈70 km long, cuts across the dominant northeast-striking structural grain of the orogen, and provides completely exposed cross-sec-

GSA Bulletin; September 1996; v. 108; no. 9; p. 1149–1166; 10 figures; 2 tables.

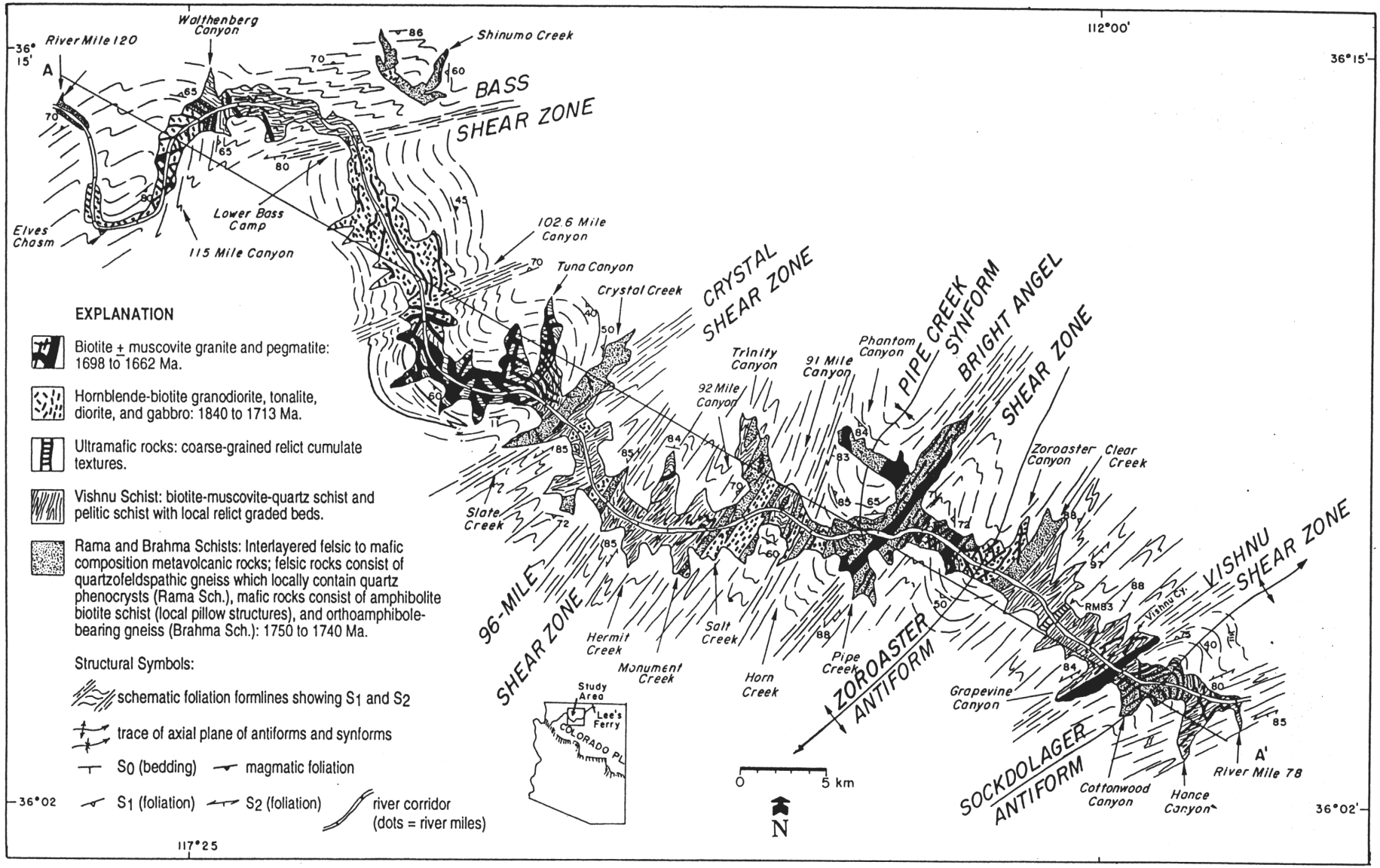

Figure 1. Simplified geologic map of Paleoproterozoic rocks in the Upper Granite Gorge, Grand Canyon. Form lines outside the Paleoproterozoic exposures show our interpretation of the trace of the regional foliation on the map surface. This map shows variably plunging kilometre-scale F_2 folds and domains of subvertical northeast-striking S_2 tectonite fabric overprinting domains of variably dipping, folded northwest-striking S_1 fabric. The transect is divided into metamorphic domains that are generally separated by shear zones. A–A′ is location of cross section in Figure 2.

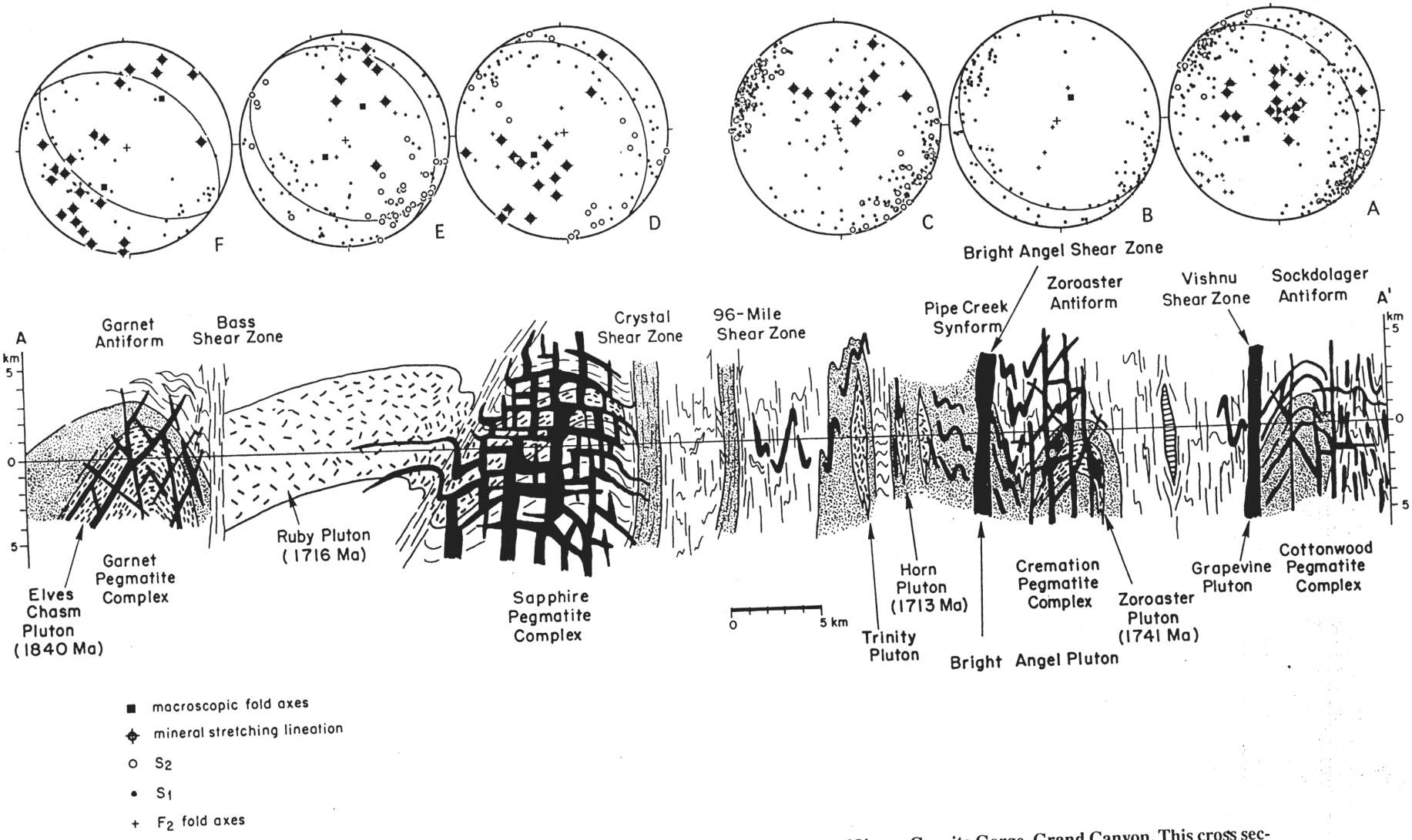

Figure 2. Geologic cross section (location shown in Fig. 1) and equal-area projections of Upper Granite Gorge, Grand Canyon. This cross section was constructed by projecting folds up and down plunge into the section line. It shows our interpretation of the macroscopic geometry of Paleoproterozoic rocks in the Grand Canyon before uplift and erosion. The section shows ≈10 km of vertical structural relief and large F_2 folds that repeat lithologies across the transect. Shear zones are typically developed on the limbs of large folds or adjacent to heterogeneities such as plutons or pegmatite dike complexes. (A) Stereonet of data from the Vishnu shear zone to the Bright Angel shear zone. (B) Stereonet of data from the Bright Angel shear zone to the Horn pluton (Phantom and Pipe Creek areas). (C) Stereonet of data from the Horn pluton to the 96-Mile shear zone area. (D) Stereonet of data from the 96-Mile shear zone to Crystal shear zone area. (E) Stereonet of data from the Bass shear zone to Waltenberg Canyon area. (F) Stereonet of data from the Waltenberg Canyon to mile 120 area.

tional views of one part of the orogen. We introduce a new lithostratigraphic nomenclature for supracrustal rocks and a revised classification of plutons. Our structural analysis of this transect, combined with geochronology and metamorphic data, provides insight into the geometry and kinematic history of deformation associated with the generation of island arcs, the juxtaposition of arc terranes, and the ultimate assembly of juvenile arc rocks to form new continental lithosphere in the Southwest. Finally, our analysis provides insight to the processes that operated in the middle crust, including the interactions of plutonism, metamorphism, and dramatic strain partitioning, at all scales, during progressive shortening.

ROCK UNITS

A new geologic map (Fig. 1) and cross section (Fig. 2) of the Upper Granite Gorge were compiled from detailed field mapping (Ilg, 1992; Ilg and Karlstrom, 1992, 1993, 1994), from photogeologic interpretation of high-resolution (1:4800 and 1:10 000) aerial photographs of the river corridor, and from previous work (Walcott, 1890, 1894, 1895; Noble and Hunter, 1916; Campbell, 1936, 1937; Campbell and Maxson, 1933–1938; Pasteels and Silver, 1965; Maxson, 1968; Ragan and Sheridan, 1970; Lingley, 1973; Walen, 1973; Livingston et al., 1974; Babcock et al., 1974, 1979; Clark, 1976, 1979; Brown et al., 1979; Billingsley et al., 1980; Huntoon et al., 1980; Babcock, 1990). This section discusses new insights regarding lithostratigraphy and the nature of protoliths.

The "Vishnu terrane" of Walcott (1894) is here named the Granite Gorge Metamorphic Suite. We recommend this name instead of "Vishnu Metamorphic Complex" (Babcock, 1990) for the entire sequence of metamorphosed volcanic and sedimentary rocks in the Grand Canyon. In our usage, the term "Vishnu Schist" is reserved for the metasedimentary rocks, following original usage (Walcott, 1890), and the term "metamorphic suite" is preferred over "metamorphic complex" (Henderson et al., 1980) because metamorphosed supracrustal rocks can be mapped separately from intrusive rocks at the scales of 1:24 000 and 1:10 000.

1.84 Ga Gneissic Basement

Numerous workers have speculated on the nature of the basement to Paleoproterozoic supracrustal rocks in the Southwest (DePaolo, 1981; Bennett and DePaolo, 1987; Wooden and Dewitt, 1991). Early studies in the Grand Canyon suggested that the quartzofeldspathic Elves Chasm Gneiss and Trinity Gneiss were basement to supracrustal rocks (Noble and Hunter, 1916). Instead, Babcock et al. (1974) suggested that the Elves Chasm and the Trinity Gneisses were formed either by the "granitization" of Vishnu Schist or that they were orthogneisses. Later, Babcock (1990) suggested that if the orthoamphibole-bearing horizon (see below) is interpreted as a paleosol, then the Elves Chasm Gneiss might be basement to the supracrustal rocks. Babcock (1990) interpreted the Trinity Gneiss to be a metamorphosed sequence of interbedded dacitic tuffs and flows and sedimentary rocks.

Our mapping and geochronologic data suggest that the Trinity Gneiss is not basement, but rather a 1730 Ma orthogneiss, intrusive into the Granite Gorge Metamorphic Suite. Some layers do have geochemical signatures consistent with a sedimentary parentage (Babcock, 1990), but we interpret these to be screens of country rock because the Trinity Gneiss is clearly intrusive into some of them (Fig. 3). However, the Elves Chasm Gneiss (Waltenberg Canyon area of Fig. 1) is likely part of the basement on which the Granite Gorge Metamorphic Suite was deposited. Hawkins et al. (1996) reported a 1840 Ma crystallization age for the Elves Chasm pluton and interpreted the Elves Chasm Gneiss as an older granodioritic pluton. The contact around this older pluton is tectonized but is defined by a high-grade orthoamphibole-bearing zone. The contact is exposed near Waltenberg Canyon, in 115-Mile Canyon, near Blacktail Canyon, and in the Middle Granite Gorge. These orthoamphibole-bearing gneisses suggest a zone of early alteration of the contact zone, possibly a metamorphosed and sheared paleosol as proposed by Babcock (1990), or possibly a zone of hydrothermal alteration. In any case, these data suggest that Penokean-Hudsonian age (1.89–1.84 Ga) basement is present in the western part of the Upper Granite Gorge.

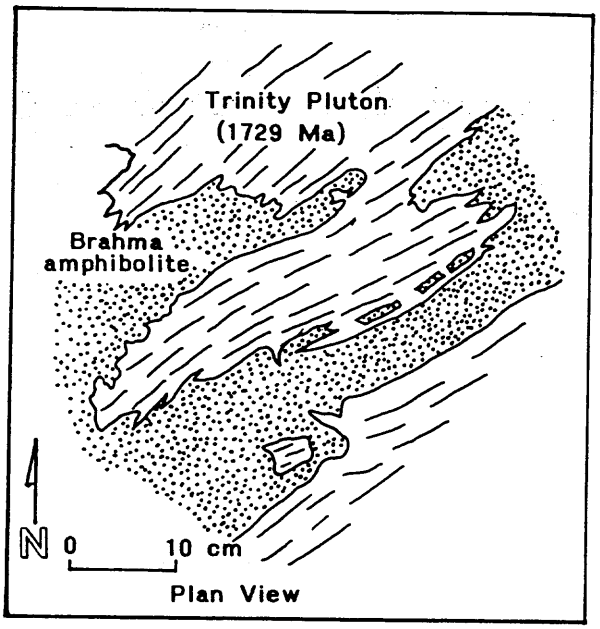

Figure 3. Field relations showing the Trinity pluton intruding the Granite Gorge Metamorphic Suite. Dashed lines in the plutonic rocks represent the trace of folded S_1 on the outcrop surface.

Granite Gorge Metamorphic Suite

The Granite Gorge Metamorphic Suite is composed of several mappable rock types (Fig. 4), although stratigraphic relationships and original thicknesses have been obscured and modified by deformation. The terms "Rama Schist," "Brahma Schist," and "Vishnu Schist" are applied to mappable units in the Upper (Fig. 1), Middle, and Lower Granite Gorges. In many areas these supracrustal rocks are the oldest rocks exposed in the Grand Canyon (cf. Hawkins et al., 1996). The metavolcanic and metasedimentary rocks are interpreted to represent marine volcanic-arc sequences locally constructed on, or juxtaposed with, older (1.84 Ga) sialic crust and intruded by 1.74–1.71 Ga plutonic rocks. Primary structures such as relict pillows and graded bedding show that the sedimentary rocks were locally deposited on the volcanic sequence and that the mafic and felsic metavolcanic rocks are commonly interlayered. However, similar volcanogenic sequences could have been deposited at different times or in separate basins, and such differences would be difficult to unravel because of subsequent tectonism. Thus, our terminology should be considered mainly lithologic, not necessarily stratigraphic.

Rama Schist. The Rama Schist[1] consists of quartzofeldspathic schist and gneiss. It is dominated by massive fine-grained quartzofeldspathic

[1]Although Maxson (1968) previously used the designation "Rama Schist" for ca. 1 Ga. basalts of the Mesoproterozoic Grand Canyon Supergroup, the name "Rama" was abandoned when these basalts were formally named the "Cardenas Basalt" (Ford et al., 1972; Lucchitta and Beus, 1987; Elston, 1989). Thus, this new usage of the term "Rama" should not be confusing.

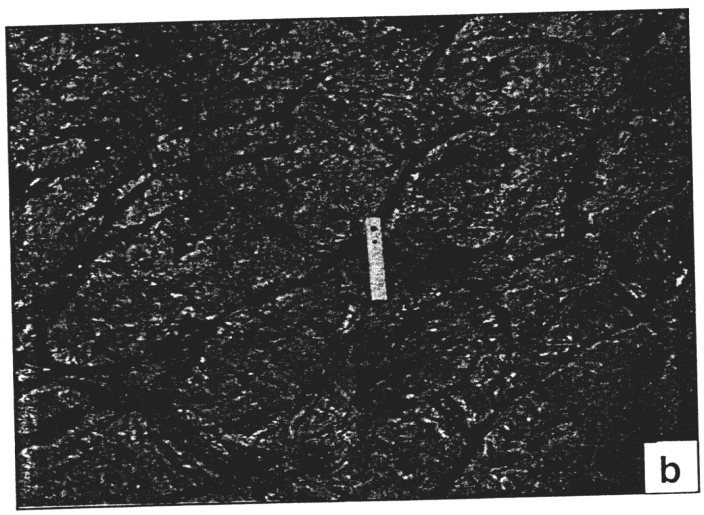

Figure 4. Lithologies of the Granite Gorge Metamorphic Suite. (a) Interlayered character of Rama and Brahma Schists from Clear Creek. In outcrop, the Rama Schist is generally massive, featureless, and highly resistant. (b) Relict pillow structures within Brahma Schist amphibolites in Shinumo Creek. Relict pillow structures are defined by calc-silicate– and hornblende-rich rinds that define triple junctions and by amygdules near the top (upper left) of the relict pillow structures. (c) Relict graded beds in Vishnu Schist meta–lithic arenites. One light-dark layer pair make up part of a relict Bouma sequence (tops to upper right). The light layers are quartz and feldspar rich, whereas the dark layers contain a high proportion of aluminous minerals such as mica, garnet, and staurolite. We have documented relict graded beds in numerous locations throughout the Upper and Middle Granite Gorges. The abundance of relict graded beds, the presence of relict pillow structures in the Brahma Schist, and the absence of coarse sedimentary protoliths suggest that Granite Gorge Metamorphic Suite protoliths were deposited in a submarine environment.

rocks that locally preserve euhedral plagioclase laths. The unit also contains metarhyolites with well-preserved quartz phenocrysts and interlayered micaceous quartzofeldspathic schists and gneisses. The Rama Schist is commonly complexly injected with pegmatite and contains leucocratic layers (e.g., in the Sockdolager antiform) that may in part reflect preferential partial melting of these rocks. Hawkins et al. (1996) have reported an age of 1742 Ma for a felsic gneiss from the Rama Schist in the eastern part of the transect. The presence of euhedral plagioclase laths in a fine-grained quartzofeldspathic matrix suggests that the protoliths of these rocks are metamorphosed felsic lapilli-crystal tuffs.

The Rama Schist is named after the Rama Shrine, located just north of the first exposure of the felsic metavolcanic rocks near the core of the Sockdolager antiform (Fig. 1). Reference sections for the Rama Schist are (1), for higher-grade quartzofeldspathic gneisses, ≈1 km downstream from Hance Canyon in the core of the Sockdolager antiform; (2), for the massive, metamorphosed lapilli-crystal tuffs, in Shinumo Creek ≈6 km from the Colorado River; and (3), for quartz-eye metarhyolite, near river mile 127.[2] The Rama is locally interlayered with the mafic Brahma Schist (Fig. 4a; see below).

Brahma Schist. The Brahma Schist consists of amphibolite, hornblende-biotite-plagioclase schist, biotite-plagioclase schist, orthoamphibole-bearing schist and gneiss, and metamorphosed sulfide deposits. These rocks were named the Brahma Schist by Campbell and Maxson (1937) and were mapped as a distinct unit by Maxson (1968). These rocks are readily mappable at 1:24 000 in most areas of the canyon, except near Phantom Ranch where the Vishnu, Rama, and Brahma Schists are complexly interlayered (Ragan and Sheridan, 1970).

The petrology and geochemistry of Brahma Schist amphibolites were studied by Clark (1976), who divided the amphibolites and mafic schists into five groups based on field occurrence and mineral assemblage: (1) anthophyllite-bearing and cordierite-anthophyllite–bearing rocks (orthoamphibole schists), (2) "early amphibolites," (3) the Granite Park mafic body (Lower Granite Gorge area), (4) hornblende-bearing dikes, and (5) tremolite-bearing dikes. We agree with Clark's interpretation that the orthoamphibole-bearing (group 1) rocks are metamorphosed, hydrothermally altered, mafic marine volcanic rocks and that the "early amphibolites" (group 2) are metamorphosed basalts and basaltic tuffs. Clark's groups 1 and 2 compose the supracrustal Brahma Schist, following Campbell and Maxson's (1938) original usage of the term.

Massive amphibolite (part of Clark's group 2) makes up 30%–40% of the Brahma Schist. This unit does not typically preserve primary igneous

[2]Geographic locations along the Coloroado River in the Grand Canyon are designated in terms of river miles downstream from Lee's Ferry, Arizona. In Figure 1, dots within the river corridor show approximate river miles, starting with mile 78; 1 mile = 1.6 km. River left refers to left shore when facing downstream, and river right refers to the right shore.

features. However, relict pillow structures are present in Clear Creek (Campbell and Maxson, 1933) and across from the mouth of Horn Creek, in 92-Mile Canyon, in Crystal Creek, in Slate Creek, in Shinumo Creek, and 100 m upstream from the mouth of Blacktail Canyon along the Colorado River (Fig. 4b). The massive amphibolites have a tholeiitic character and trace element compositions consistent with an island-arc environment (Clark, 1976).

Biotite + plagioclase schist and hornblende + biotite + plagioclase schist (the remainder of Clark's group 2) make up ≈50% of the Brahma Schist in the Upper Granite Gorge. Strong tectonic layering has obscured primary igneous textures in most locations. However, original textures are preserved in several locations (e.g., along the river trail between the Kaibab and Bright Angel bridges), where subangular quartz + plagioclase + biotite fragments are entrained in an amphibolitic matrix, suggesting that some of these rocks may have been volcaniclastic breccias. Interlayered with the biotite schist are discontinuous metre-scale lenses of garnet + diopside + epidote + calcite rocks. The protoliths of these lenses are possibly relatively thin layers of a calcareous shale (Campbell and Maxson, 1933) or algal mats interbedded with submarine sediments (Babcock, 1990).

The Brahma Schist also contains exposures of orthoamphibole-bearing rocks (Clark's group 1). Examples are exposed just below Waltenberg Canyon, near mile 115 on river left, near Blacktail Canyon, and near mile 127 in the Middle Granite Gorge. Smaller, isolated exposures occur in Bright Angel Creek, Pipe Creek, and Hermit Creek. These rocks are characterized by gedrite + anthophyllite + cordierite + cummingtonite + biotite + garnet assemblages. They are interpreted to be hydrothermally altered, mafic marine volcanic rocks (Vallance, 1967).

The presence of relict pillow basalt, orthoamphibolite rocks, and associated sulfide mineralization indicates that the Brahma Schist was the product of dominantly mafic submarine volcanism. Large-scale interlayering of mafic to intermediate composition (Brahma) and felsic (Rama) volcanic rocks (Fig. 4a) is similar to that found in the Yavapai Supergroup of central Arizona (Condie, 1986; Darrach et al., 1991). A quartz + plagioclase phenocrystic felsic metavolcanic rock interlayered with Brahma Schist rocks near the mouth of Clear Creek yields a crystallization age of 1750 Ma (Hawkins et al., 1996). We interpret this age and the 1742 Ma age from a sample of gneiss from the Rama Schist to represent the approximate ages for the mafic-felsic Rama-Brahma package, which is nearly identical in age to the 1750–1740 Ma Yavapai Supergroup of central Arizona (Karlstrom and Bowring, 1993).

Vishnu Schist. The Vishnu Schist consists of pelitic schist and quartz + biotite + muscovite schists interpreted as meta–lithic-arenites, metagraywackes, and calc-silicate lenses and pods. Meta–lithic-arenite and metagraywacke sequences show thick sections (kilometre-scale) of rhythmically banded (centimetre- to metre-scale) coarser and finer layers, with locally well-preserved bedding and graded bedding (Walcott, 1894; Clark, 1976; Fig. 4c). Locally, the Vishnu Schist contains pelitic and semipelitic schists that variably contain andalusite, sillimanite, staurolite, chloritoid, cordierite, and garnet. Original grain size in the Vishnu Schist metasedimentary rocks probably ranged from medium-grained sand to silt and clay. Conglomerates are conspicuously absent in the Vishnu metasedimentary rocks (Campbell and Maxson, 1933). Relict graded bedding (Fig. 4c), association with metavolcanic rocks containing pillow structures (Fig. 4b), lack of coarse sediments, and geochemical data (Babcock, 1990) indicate that the metasedimentary units accumulated in an oceanic island-arc environment, as suggested for the Yavapai Supergroup rocks of central Arizona (Anderson and Silver, 1976; Bowring and Karlstrom, 1990).

The contact between the Vishnu Schist and the Brahma Schist is generally concordant, and the rocks are interlayered as in Clear Creek, ≈1 km from the Colorado River. A reference section for the Vishnu Schist is in Vishnu Canyon. Other easily accessible exposures of Vishnu Schist metasedimentary rocks occur (1), for highest-grade Vishnu rocks, along the river between mile 78 and Hance Canyon; (2), for lowest-grade Vishnu rocks, between Vishnu Canyon and Clear Creek, near 91-Mile Canyon, from Monument Canyon to 96-Mile Canyon, and from 96-Mile Canyon to Crystal Creek; and (3), in isolated septa, from Crystal Creek to mile 102.6 and from Lower Bass Camp to Waltenberg Canyon (Fig. 1). In the latter area, metasedimentary rocks with graded bedding clearly overlie metavolcanic rocks. As with the metavolcanic rocks, we expect that the Vishnu Schist may be further divisible in the future into different units and/or originally disparate tectonic packages juxtaposed across shear zones. However, present understanding of the stratigraphy and structure does not suggest obvious further subdivision.

Plutonic Rocks

The Granite Gorge Metamorphic Suite is intruded by Paleoproterozoic granitoid plutons, mafic dikes, and granitic pegmatite dike swarms that together make up about one-half of the Paleoproterozoic rocks exposed in the Upper Granite Gorge (Fig. 1). Clark (1976) named these rocks the "Zoroaster Plutonic Complex," modifying the term "Zoroaster Granite" (Maxson, 1968), which in turn was modified from the original "Zoroaster Gneiss" (Campbell and Maxson, 1933). However, in the Upper Granite Gorge, these granitoids have a range in *age* of at least 1840–1662 Ma (Hawkins et al., 1996), in *composition* from gabbro to granite, in *morphology* from large plutons to stocks to dikes and sills, and in *tectonic significance* from volcanic arc–related plutons to syncollisional plutons to postdeformational dikes and sills. Thus, following Henderson et al. (1980), we suggest that the name "Zoroaster Plutonic Complex" should be replaced with compositional and temporal designations.

We retain geographic names for individual plutons (following Lingley, 1973; Walen, 1973; Clark, 1976; and Babcock, 1990), propose new names for major pegmatite and/or granite dike swarms (Fig. 2), and propose a twofold classification of plutons: (1) 1.74–1.71 Ga plutons and plutonic complexes that are generally mafic to intermediate composition, ≥100 m scale, and of probable arc affinity and (2) 1.70–1.66 Ga granitic and granitic pegmatite dikes and dike complexes that are probably related to the collisional assembly of the orogen. This subdivision is similar to one proposed for central Arizona (Karlstrom and Bowring, 1993) and differs from the subdivision of Babcock (1990) because we place less reliance on the inferred timing of granitoid emplacement relative to deformation.

1.74–1.71 Ga Plutons. In this group are included the Zoroaster, Pipe Creek, Horn Creek, Trinity, Boucher, Crystal, and Ruby plutons and possibly parts of the Elves Chasm pluton (Fig. 2). This group of plutons is similar to the Ruby Creek superunit of Babcock (1990). The compositions of these plutons range from hypersthene gabbro (Noble and Hunter, 1916) to quartz diorite to tonalite and granodiorite. The bodies are typically sheetlike and concordant with early foliation (S_1). They show variable degrees of fabric development. For example, the 1741 Ma Zoroaster and 1730 Ma Trinity plutons are strongly foliated and define large folds (Figs. 1 and 2) whereas the nearly unfoliated 1717 Ma Ruby pluton preserves tectonic fabric only on its eastern margin. Well-documented intrusive relationships between this suite of plutons and the Granite Gorge Metamorphic Suite have been observed for the Zoroaster, Phantom, Pipe Creek, Horn Creek, Trinity (Fig. 3a). Boucher, and Ruby plutons. However, some contacts are tectonic, e.g., the west margin of the Ruby pluton near Bass Camp (see Fig. 1) and the east margin of the Boucher pluton near 96-Mile Canyon. Available geochemical data show low initial Sr isotope ratios and major and trace element data consistent with an island-arc origin (Clark, 1976; Babcock, 1990).

We have identified several distinctive ultramafic bodies (Fig. 1), some of which were previously mapped as 1.1 Ga diabase dikes (e.g., Huntoon et al., 1980). However, most of these bodies are ductilely deformed, and they are locally crosscut by pegmatite dikes (e.g., in a tributary to Crystal Creek) of probable Paleoproterozoic age. These ultramafic bodies may be tectonic slivers of the cumulate rocks of the more evolved arc plutons and/or tectonic slivers of part of an ophiolite sequence.

1.70–1.66 Ga Granites and Pegmatites. These granitoids have a fundamentally different composition, intrusive style, and deformational character than the older, volumetrically larger, mafic to intermediate-composition plutons. Most of these rocks are true granites and occur as somewhat smaller plutons, stocks, injection zones, and pegmatite complexes (black units in Figs. 1 and 2). The granites consist of quartz, K-feldspar, plagioclase (An_2–An_{20}), and muscovite and/or biotite, garnet, and rare hornblende. U-Pb ages are 1698–1662 Ma (Hawkins et al., 1996).

Networks of dikes containing subequal volumes of gradationally related pegmatite and granite occur in major swarms within the Upper Granite Gorge (Figs. 1 and 2). These intrusive complexes are here named the Cottonwood, Cremation, Sapphire, and Garnet Canyon pegmatite complexes (Fig. 2). Pegmatite and granite dike networks locally compose one-half or more of the rock volume, in which case the proportion of dike to country rock is such that they could be designated plutons (e.g., the Sapphire pegmatite complex) although they clearly coalesced from individual dikes. Individual tabular pegmatite dikes range from nearly undeformed to isoclinally folded (Fig. 5). Dikes are locally concordant to regional foliation or may abruptly truncate foliation and may occur in orthogonal networks (Fig. 5d). Thus, in contrast to early plutons whose geometry is that of large folded sheets, the late pegmatites record emplacement of dikes during brittle fracturing of country rock in an overall ductile shortening regime (Davidson et al., 1994).

STRUCTURAL GEOLOGY AND DEFORMATIONAL HISTORY

This section reviews the structural geology of the Upper Gorge transect (Fig. 1) and builds upon the structural studies done by Lingley (1973), Walen (1973), and Brown et al. (1979). These workers documented several fold generations based on mesoscopic overprinting relationships, including an early compositional tectonic layering (S_1), a second-generation

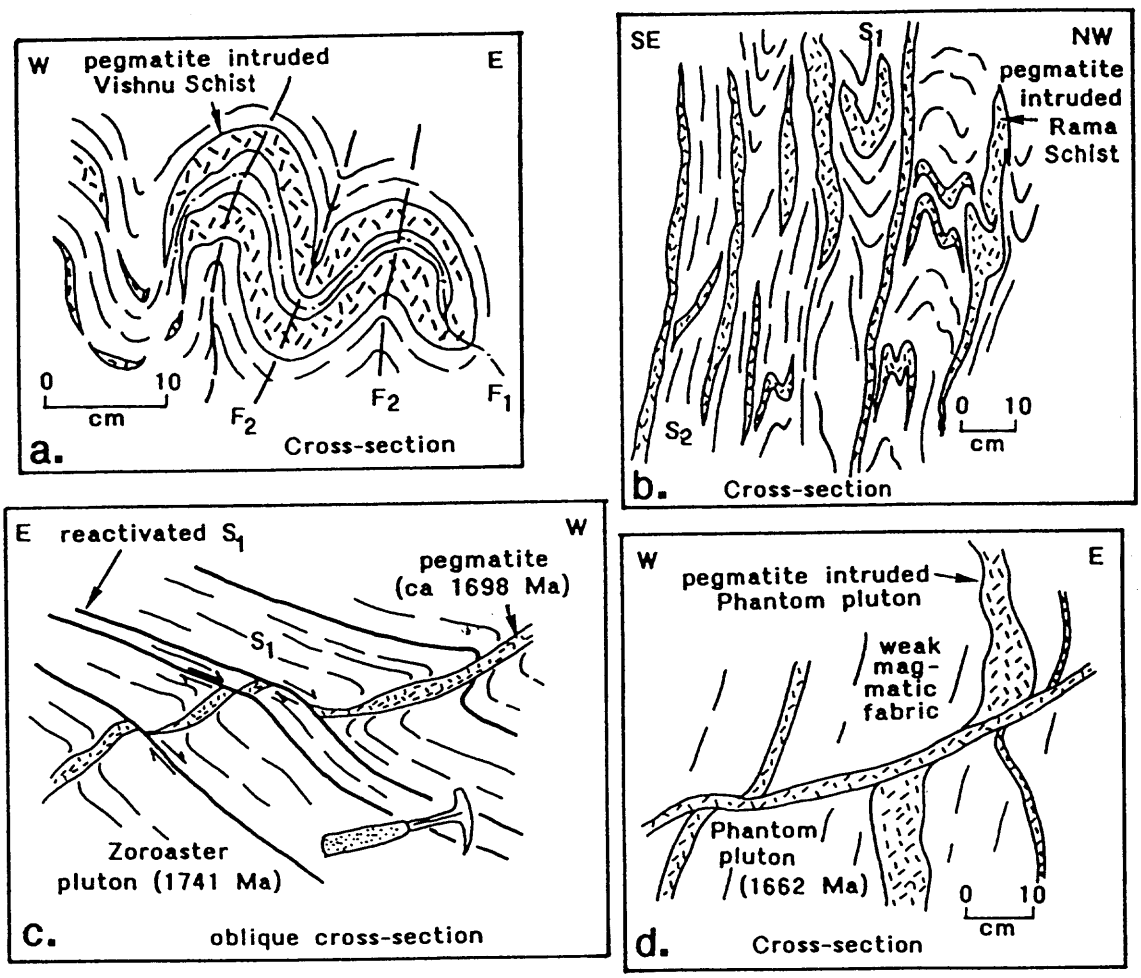

Figure 5. Sketches showing variable relationship of pegmatites to deformation. Individual pegmatite dikes range in age from 1698 to 1662 Ma, are isoclinally folded by F_1 (a), are boudinaged in S_1 microstructures (a), form F_2 folds with S_2 axial-planar cleavage (a and b), are boudinaged in S_2 (b), crosscut S_2 with mylonites developed in their cores (see Fig. 8c), crosscut S_2 (see Fig. 7), are slightly deformed along reactivated S_1 (c), and form essentially undeformed orthogonal dike networks (d). Combined with the fact that the 1685 Ma pegmatites record little shortening, these observations indicate that most of the deformation occurred in the interval 1700–1685 Ma. However, pegmatites that crosscut the 1662 Ma Phantom pluton (d) show displacement on their margins, indicating less intense, but continued deformation.

vertical cleavage (S_2), and late-stage kinks and crenulations (S_3). We extend their analysis by correlating these fold and fabric generations across the entire transect, by identifying the geometry of major folds and shear zones, by proposing a kinematic framework for observed fold generations, and by defining the timing and interrelationships of deformation, metamorphism, and plutonism.

The Upper Granite Gorge transect is dominated by a heterogeneously developed, subvertical northeast-striking foliation (S_2; Figs. 1 and 2) with moderate to steeply plunging stretching lineation (L_2; Fig. 2). Transposition of rock units within this vertical foliation is intense, and stratigraphic relationships are obscured. Although this vertical fabric clearly dominates the transect, our cross section (Fig. 2) shows a relatively simple macroscopic geometry characterized by (1) domains of preserved, shallowly dipping, penetrative S_1 tectonic layering that are variably transposed by S_2; (2) 10-km-wavelength upright F_2 antiforms and transposed synforms; (3) repetition of major rock packages across strike; and (4) shear zones that are localized on fold limbs and adjacent to rock contacts. Later generations of structures such as S_3 kinks and crenulation cleavages accommodated additional shortening but did little to affect this macroscopic geometry.

Three generations of structures are identified primarily on the basis of overprinting in individual outcrops (Hobbs et al., 1976, Chapter 8). These specific generations of structures can be correlated across the transect (see Williams, 1985) on the basis of style and orientation. *Group 1* structures predate the dominant, northeast-striking, subvertical foliation (Fig. 1) and include a penetrative S_1 foliation and several generations of F_1 folds. *Group 2* structures are those fabrics related to the dominant, highly partitioned, subvertical, northeast-striking cleavage and include F_2 upright folds and associated subvertical S_2 foliation and northeast-striking, subvertical shear zones. *Group 3* structures overprint group 1 and 2 structures and include a wide variety of kinks and incipient crenulation cleavages (see Fig. 8). We do not use the D_1, D_2, D_3 terminology because groups of structures may themselves record multiple events or different groups may be part of a single progressive-deformation event (e.g., Williams and Zwart, 1977).

Group 1 Structures

Group 1 structures include a penetrative tectonite fabric (S_1) and several generations of interfolial folds and nappes of S_1 (Fig. 6, a, b, c). In thin section, S_1 varies in morphology, in part depending on lithology. In amphibolites, S_1 is dominantly a schistosity defined by elongate amphiboles and by the shape-preferred orientation of biotite, quartz, and feldspar. In felsic metavolcanic rocks, it is more commonly a gneissic layering that is defined by compositional layering of alternating mica, quartz, and feldspar and by the alignment of pegmatitic leucosomes. In metasedimentary schists, S_1 is preserved as compositional layering within microlithons and fold-hinge regions. When preserved, S_1 is defined by shape-preferred orientations of biotite, muscovite, quartz, and feldspar in the lower-grade areas and by sillimanite and biotite in the higher-grade areas. Even where S_2 has nearly completely overprinted S_1, earlier foliations can often be seen as straight inclusion trails in porphyroblasts over a large area (e.g., Aerden, 1995; Ilg, unpublished data).

S_1 layering (schistose and gneissic) is axial planar to one or more generations of F_1 folds (Fig. 6, a, b, c) found throughout the transect as mesoscopic, commonly intrafolial folds deformed by later structures. Well-preserved macroscopic F_1 folds are exposed in the Shinumo Canyon to Waltenberg Canyon area (see Fig. 1 form lines and Fig. 6c). Hinge lines of F_1 folds are commonly rotated toward the L_2 stretching lineation direction in domains of strong S_2 development. However, in northwest-striking foliation domains (e.g., Waltenberg Canyon), F_1 fold axes plunge shallowly westward to northward. Unmodified L_1 is rare because most S_1 surfaces were reactivated by S_2 (Fig. 5c). However, in amphibolites, L_1 is defined by hornblende crystals and is locally folded around F_2 folds (particularly between Clear Creek and Zoroaster Canyon).

Figure 6. Schematic deformation-progression diagram (center) for group 1 and group 2 structures with examples from outcrop photos. As shown in the schematic diagram, these diverse structures are interpreted to record both the sequence of development of structures in group 2 domains and the strain heterogeneity across the transect. (a) Thrust nappe developed in Ruby pluton phases shows a relatively unmodified group 1 structure. (b) Recumbent isoclinal F_1 folds of S_0 in Vishnu Schist are also typical of relatively unmodified group 1 structures. (c) Refolding of an F_1 fold of Vishnu Schist meta–lithic-arenites; these structures are common in the Shinumo Canyon to Waltenberg Canyon area. (d) F_2 fold with axial-planar cleavage developed in metasedimentary rocks but not in amphibolite. (e) Advanced S_2 development in Clear Creek.

The details of the kinematic history and strain magnitude associated with group 1 structures remain obscure because of intense overprinting by group 2 structures. The 1741 Ma Zoroaster and 1730 Ma Trinity plutons show strong folded S_1 fabrics and have been called gneisses (Campbell and Maxson, 1933; Lingley, 1973; Babcock, 1990). The 1717 Ma Ruby and 1713 Ma Horn plutons show little evidence for S_1-related solid-state deformation although northwest-striking magmatic layering or weak tectonic layering (alignment of feldspar phenocrysts) is present. S_1 is crosscut by dikes as old as 1698 Ma and thus had clearly ceased forming by that time. These timing relationships indicate that most S_1 strain probably accumulated in the interval 1730–1713 Ma, although continued movement on S_1 fabrics may have continued to ca 1.7 Ga.

Group 2 Structures

Group 2 structures include a penetrative but heterogeneously developed, subvertical, northeast-striking schistosity or spaced (0.5 cm) crenulation cleavage (S_2) that is associated with upright to asymmetric (west-dipping axial planes) and open-to-isoclinal F_2 folds (Fig. 6).

S_2 is strongly partitioned into high- and low-strain domains at many scales. S_2 foliation varies in morphology depending on strain intensity and rock type. For example, in amphibolites folded by the Zoroaster antiform, S_2 is not developed as an axial planar cleavage; however, S_1 foliations were reoriented and reactivated by S_2 shearing and flattening during F_2 folding. Thus, throughout much of the transect, S_2 is commonly a composite S_1-S_2 foliation whose northeast-striking orientation reflects S_2 strain but whose morphology reflects the combined effects of the folding of S_1 by F_2 folds, shearing of S_1 on F_2 fold limbs, and S_2 development. In contrast, in metasedimentary rocks, S_2 is a differentiated crenulation cleavage to penetrative schistosity in which S_2 is defined by a new alignment of micas and sillimanite in high-temperature domains, by shape-preferred orientation of chlorite, and by alignment of epidote-group minerals in low-temperature domains.

Well-documented macroscopic (kilometre-scale) F_2 folds (Fig. 1) include the Sockdolager antiform (Fig. 2, stereonet A, plunge of 36° to 45°), the Zoroaster antiform (Fig. 2, stereonet B, plunge of 44° to 226°; see also Lingley, 1973), the Pipe Creek synform (plunge of 78° to 35°), and the Sapphire antiform (this structure is too large and complex to describe with a single trend and plunge). Other macroscopic folds shown in Figure 2

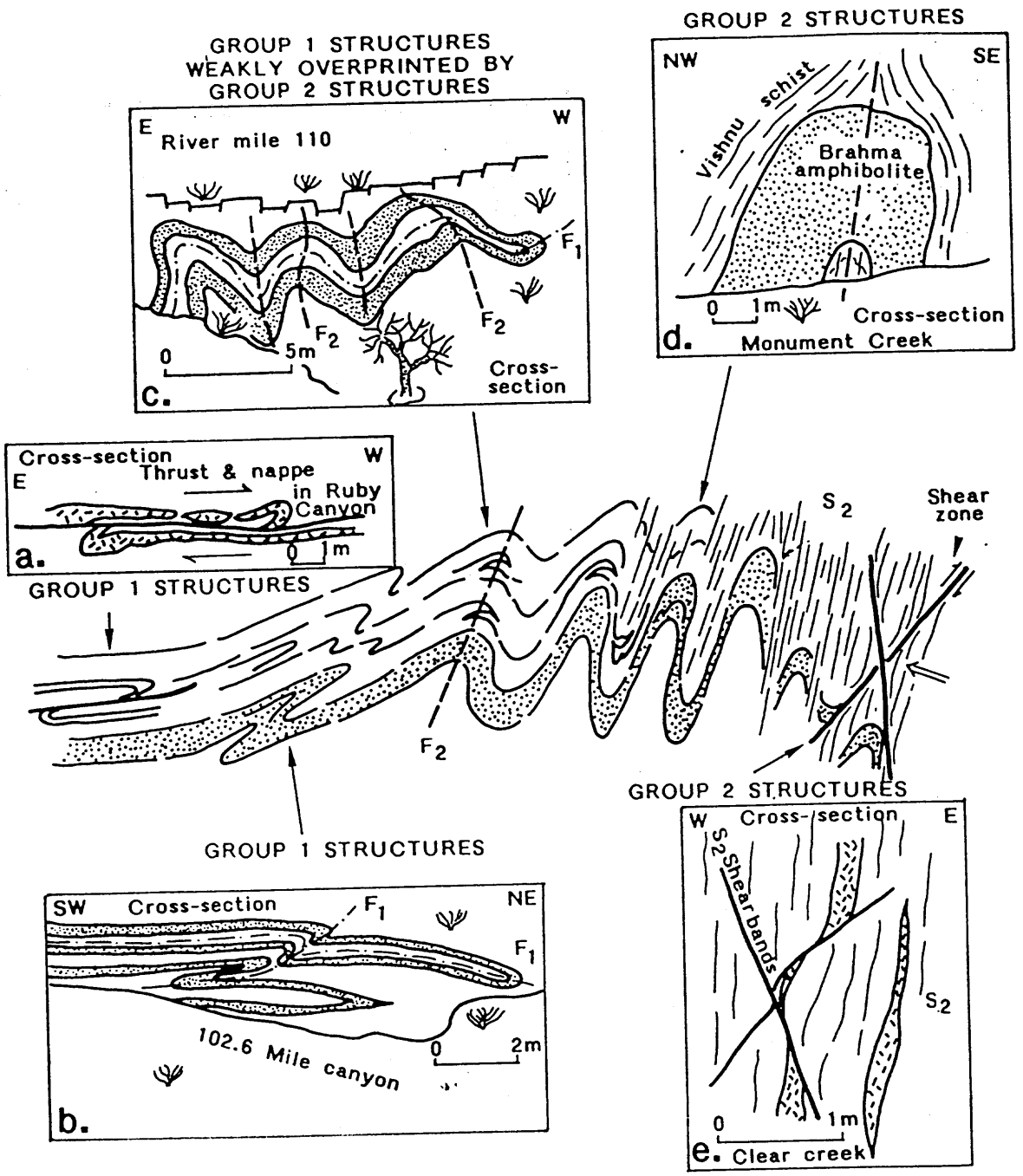

(e.g., Mile 86 synform) are less well defined because inferred hinge regions are transposed. Figures 1 and 2 provide a geologic overview of group 2 structures.

L_2 is moderately to steeply plunging on S_2 (Fig. 2 stereonets A, C, D) and is defined by amphibole, sillimanite, and feldspar. The variable plunge of L_2 stretching lineations reflects the rotation of L_1 lineations on S_1-S_2 composite foliation toward subvertical extension during S_2 formation. This pattern is compatible with pervasive subvertical boudinage of layers and intrusive rocks within the S_1-S_2 foliation. Curvilinear hinge lines of F_2 folds are seen in individual mesoscale folds and are also reflected by variation in the orientation of macroscopic fold-hinge lines (see Fig. 2, stereonets A, B, D).

Timing of the formation of group 2 structures is relatively well defined. S_2 is present in a 1698 Ma granite stock that crosscuts S_1 in the core of the Zoroaster antiform (Fig. 2). A 1697 Ma dike crosscuts S_1 and is folded by an F_2 fold near mile 111. S_2 is crosscut by weakly buckled to undeformed 1685 Ma granite and pegmatite dikes (Fig. 7). These timing relationships indicate that most of the regional S_2 shortening deformation took place in the interval 1700–1685 Ma.

Group 3 Structures

Group 3 fabric elements are diverse in character and probably represent several styles and periods of deformation that accommodated continued,

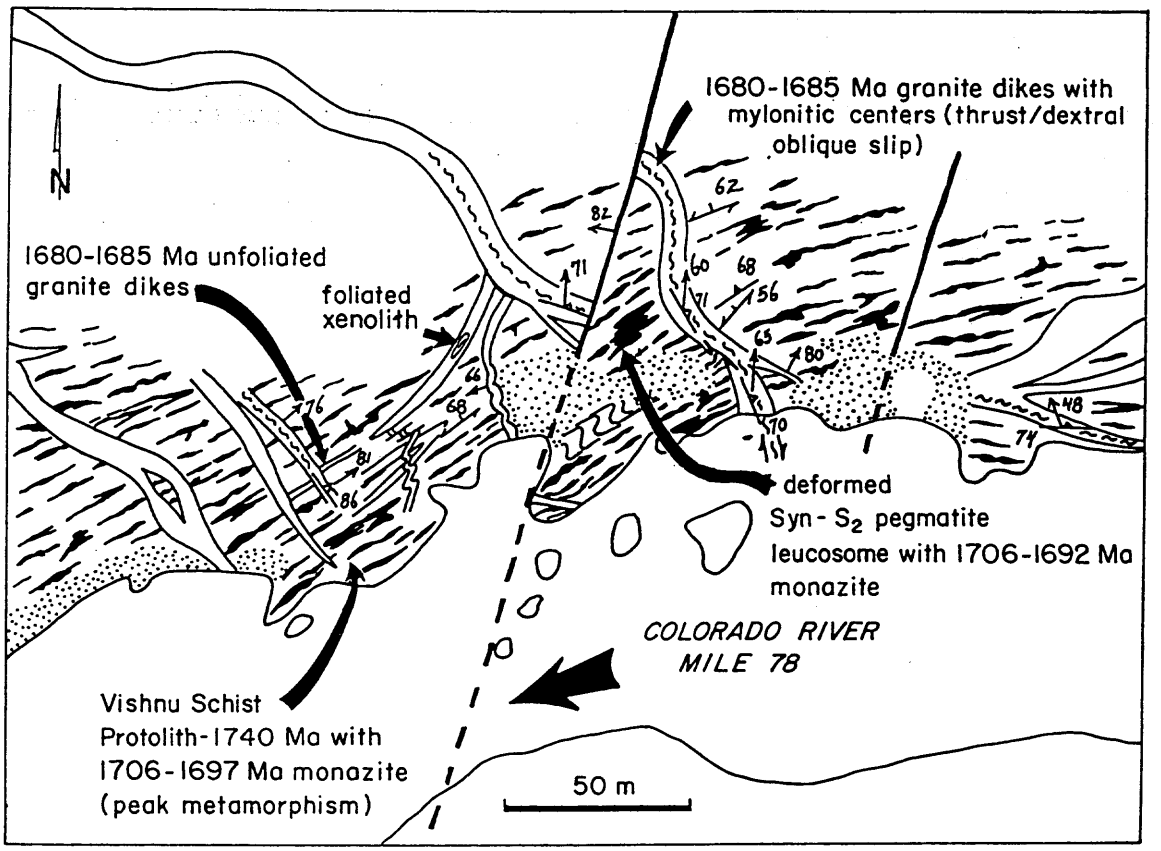

Figure 7. Detailed outcrop map for the 78-Mile area shows the timing relationships of late pegmatite dikes to regional shortening deformation. The black pattern shows weakly deformed dikes that crosscut S_2 and deformed leucosomes (shown schematically) in the migmatitic country rock.

but less intense, shortening strain (Fig. 8). S_3 crenulation cleavages generally define two orientations: east striking and vertical, and northwest striking and variably dipping. Mylonite zones in northwest-striking dikes show west-side-up dextral shear whereas east-striking dikes record dominantly dip-slip thrust motion (see Fig. 8). Dikes as young as 1682 Ma have synemplacement mylonite zones in their centers (miles 78–80). If considered together, these diverse structures and fabric elements record a kinematic regime in which shortening was subhorizontal and north-south (Fig. 8). The 1662 Ma Phantom pluton is crosscut by dikes that accommodated slip on their margins (Fig. 5d), indicating that deformation was still active at 1662 Ma. Thus, we tentatively link group 3 structures to continued deformation whose principal shortening axis rotated from being predominantly northwest-southeast directed during group 2 time to being predominantly north-south directed during group 3 time. Dated igneous rocks recording this kinematic regime are younger than 1685 Ma. It is interesting that post–main-shortening (i.e., post-S_2) dikes show no systematic orientation (i.e., the near-random distribution shown in the stereonet of Fig. 8d), suggesting that magmatic pressures were locally greater than regional stresses (Brisbin, 1986) and that group 3 structures formed at relatively low differential stresses.

S2-Parallel Shear and Fault Zones

Five major northeast-striking shear and fault zones divide the transect into blocks. These are the Vishnu (Brown et al., 1979), Bright Angel, 96-Mile, Crystal (Walen, 1973), and Bass shear zones (Fig. 1). The shear zones are typically developed on the limbs of large antiforms or synforms or against the margins of major pegmatite complexes and plutons (Fig. 2). Most zones moved after peak metamorphism and probably have multiple movement histories. In spite of similarities, each of these zones is unique in terms of geometry and metamorphic history. Phanerozoic slip on these zones is on the order of 10s to 100s of metres as indicated by the offset of the 1300–800 Ma Grand Canyon Supergroup rocks (Huntoon et al., 1980; Elston, 1989). Thus, they are pre–1.3 Ga, but timing of movements in these zones is poorly understood. Some may be important earlier group 1 shear zones (e.g., Crystal), later folded and reactivated during peak shortening.

Vishnu Fault Zone. The northeast-striking Vishnu Creek fault zone (Brown et al., 1979) is exposed in Vishnu and Grapevine Canyons (Fig. 1). A thin (10s of m) deformed coarse-grained to pegmatitic granite, the Grapevine Camp pluton, separates migmatitic (sillimanite + K-feldspar)–bearing, upper amphibolite–facies Vishnu Schist on the east from lower to middle amphibolite–facies Vishnu Schist on the west and thus represents a temperature discontinuity of ≈100–150 °C. The western margin of the pluton is cut by a Phanerozoic brittle fault with ≈12 m of offset (Huntoon et al., 1980) that reactivates the Vishnu fault. The fault truncates gneissic layering in the pluton and east-facing graded-bedding sequences in the Vishnu Schist and shows apparent dextral bending of pegmatites and S_2 into the zone. The northeast end of the zone shows brittle-ductile S-C fabric shear-sense indicators that document dextral shear at relatively low temperature. Gneissic layering in the granite appears to be defined by an annealed mylonite texture with quartz ribbons and feldspar layers. Thus, the Vishnu zone may also have an earlier high-temperature movement history.

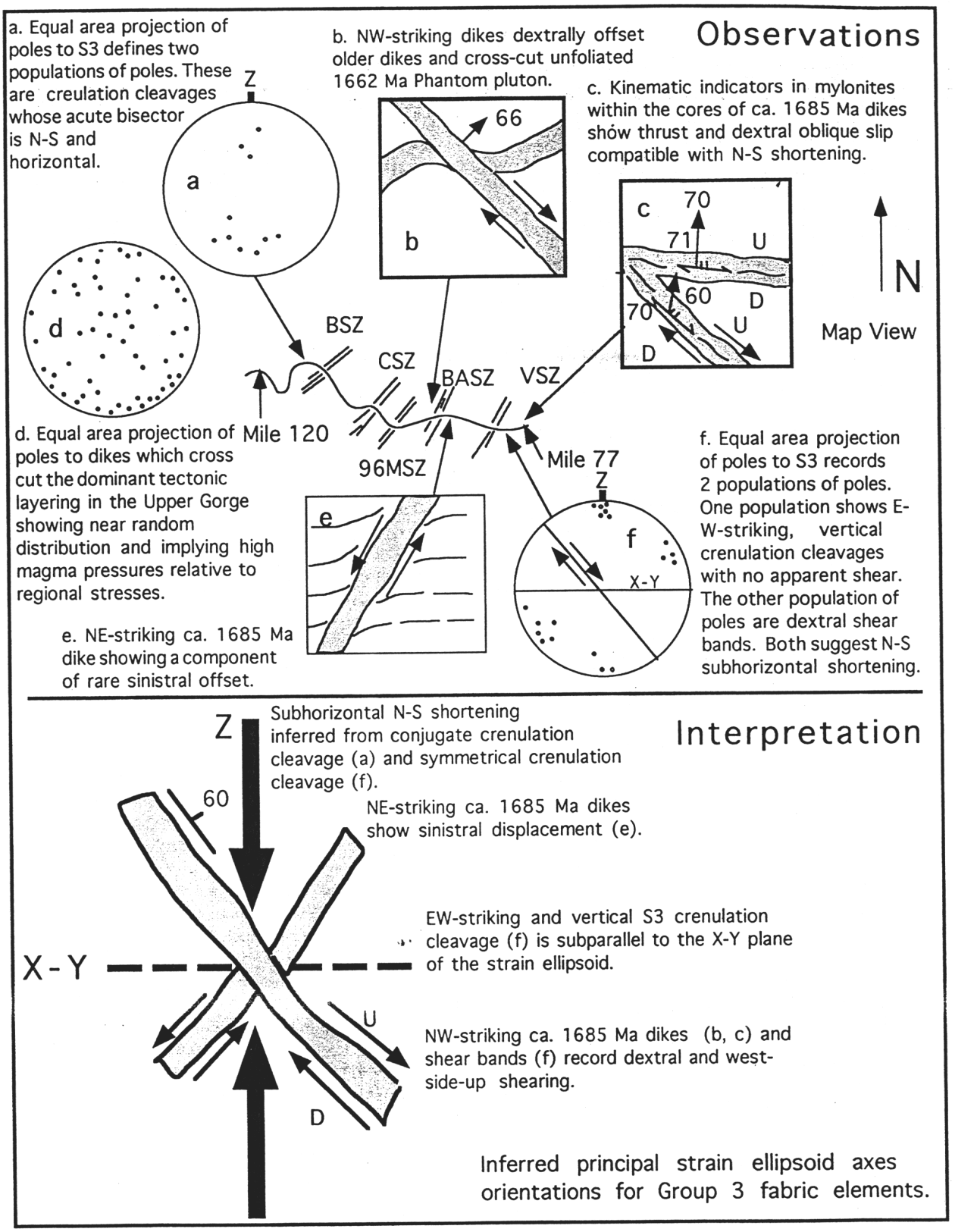

Figure 8. Diverse group 3 fabric elements may record a single strain field characterized by north-south shortening (z-axis of the strain ellipsoid). Abbreviations: VSZ—Vishnu shear zone, BASZ—Bright Angel shear zone, 96MSZ—96-Mile shear zone, CSZ—Crystal shear zone, and BSZ—Bass shear zone.

Based on brittle-ductile character and post–peak-metamorphic character of the granite, we infer that it last moved ductilely between 1.68 and 1.3 Ga.

Bright Angel Shear and Fault Zone. The Bright Angel shear zone crops out in Bright Angel Canyon (Walen, 1973) and in Pipe Creek. It is a wide zone of intense penetrative northeast-striking fabric that truncates and transposes domains of northwest-striking fabric to the west and east. As in the Vishnu shear zone, a distinctive northeast-trending pegmatitic granite (the Bright Angel pluton) appears to have intruded along a narrow zone. This pluton is interpreted to be a late synkinematic intrusion because it consists of variably foliated granite dikes and irregular granite stocks that injected the intense northeast-striking foliation of the country rock. The kinematic history of the Bright Angel shear zone is poorly understood although a component of dextral slip is inferred from the macroscopic bending of S_1 on the west side of the zone (Fig. 1). Movement apparently took place at high temperature, as shown by high-temperature solid-state fabrics in some layers that are parallel to magmatic layering in others. The long history of reactivation along this northeast-striking discontinuity (Sears, 1973; Shoemaker et al., 1978; Naeser et al., 1989), including Mesoproterozoic, Late Cretaceous–early Tertiary, and middle Tertiary displacements, suggests an important crustal boundary.

96-Mile Shear Zone. The northeast-striking 96-Mile shear zone (Walen, 1973) crops out in 96-Mile Canyon in a 300-m-wide zone of metavolcanic and metasedimentary rocks that include cherts, chloritized relict pillow breccias, and metadacites. Rocks in this zone display extreme grain-size reduction, ribboned quartz, and brittlely deformed feldspar porphyroclasts. A highly deformed metadacite defines the eastern margin of the movement zone whereas the western margin is bounded by the Boucher pluton. Garnets within the zone are brittlely deformed, with cracks filled by retrograde chlorite and epidote-group minerals. Stretching lineations have variable orientations, both downdip and shallowly plunging; and kinematic indicators record dextral strike-slip and west-side-up dip-slip motion. The 96-Mile shear zone separates an upper amphibolite–facies pelitic schist of the Vishnu Schist on the east from greenschist-facies meta-arenite of the Vishnu Schist to the west (Brown et al., 1979). The juxtaposition of metamorphic grades and fractured garnets filled with retrograde assemblages suggests that movement outlasted peak metamorphism.

Crystal Shear and Fault Zone. The Crystal shear zone is a zone of northeast-striking fabric in Crystal and Slate Creek Canyons that truncates northwest- and east-striking fabrics. Mylonitic rocks are well developed, with stretching lineations plunging steeply to the west. The zone itself is developed in lithologically heterogeneous rocks characterized by metamorphosed sulfide deposits, slices of granodioritic rocks, brecciated relict pillow structures, mylonitized felsic metavolcanic rocks, and mafic dikes, all hosted by chloritic schist. Anastomosing foliation and lenticular boudins of diverse lithologies resemble tectonic melange rocks. Although the kinematic history for early deformation is poorly understood, relative displacement is inferred to be west-side-up on the basis of macroscopic fold relationships and an apparent metamorphic pressure gradient across the zone (see below). Several pegmatite dikes (undated but similar to 1.68 Ga generation dikes) crosscut the zone in Slate Creek, suggesting that movement ceased by ca. 1.68 Ga. These geometries and timing relationships indicate that movement postdated peak-metamorphic pressures. The zone was reactivated with movements of 10s of metres during the Phanerozoic (Huntoon et al., 1980).

Recent isotopic work (Hawkins et al., 1996) shows a change in Pb isotope systematics from east to west across a possible boundary in the area of the Crystal shear zone. The presence of more radiogenic common-Pb signatures, 1840 Ma basement, and inherited zircons older than 1.8 Ga to the west (Hawkins et al., 1996) suggests that the Crystal shear zone may be an important early tectonic boundary. This interpretation is supported by the presence of metamorphosed melangelike rocks in the Crystal shear zone.

Bass Shear Zone. The east-northeast–striking Bass shear zone crops out between Upper and Lower Bass Camps (miles 107.8–108.2) in Vishnu Schist metasedimentary rocks adjacent to the internally undeformed western margin of the Ruby Pluton (Fig. 1). Dextral west-side-up kinematic indicators in a 0.5-km-wide zone within metasedimentary rocks adjacent to the pluton indicate shearing against the pluton margin. The zone is characterized by anastomosing shear bands surrounding sigmoidal foliation pods. The rocks are high grade, as indicated by the presence of sillimanite and K-feldspar, but movement apparently continued at cooler conditions as shown by pervasive chlorite, sericite alteration, and the semipenetrative brittle to ductile character of deformation. We interpret the Bass shear zone to have accommodated shortening and shearing against the rheologically competent Ruby pluton.

METAMORPHISM

Metamorphic assemblages vary across the Upper Granite Gorge, reflecting differences in bulk composition and peak-metamorphic conditions (Babcock, 1990). In general, domains with upper greenschist– to lower amphibolite–facies assemblages alternate with domains containing upper amphibolite– or granulite-facies rocks. The lower-grade assemblages typically have garnet, biotite, chlorite, and muscovite whereas the higher-grade assemblages have garnet, sillimanite, and biotite, typically with migmatitic textures. Mafic rocks at both grades have chlorite, hornblende, plagioclase ± garnet, orthoamphibole, and cordierite (Clark, 1976). On the basis of mineral assemblages and the calculated *P-T* estimates, the Upper Gorge can be divided into at least five metamorphic domains (Table 1). The lower-grade domains (e.g., miles 96–98) are interpreted to record near-ambient peak-metamorphic conditions of ≈500 °C at 6 kbar (Fig. 9c); the higher-grade areas record peak-metamorphic conditions of ≈650–725 °C at 6 kbar (Fig. 9f) and are generally associated with regions intruded by pegmatite dikes.

Compositions and textures of metamorphic porphyroblasts vary, typically as a function of metamorphic grade, along the transect, and most of the rocks contain appropriate assemblages for quantitative thermobarometry. Figure 9 compares a typical amphibolite-facies schist from mile 83.8 (sample K3-83.8) with a typical lower granulite–facies schist from mile 78.9 (sample K3-78.9). Amphibolite-facies garnet tends to be euhedral with prograde compositional zoning. Pyrope (and Mg ratio) increases (Fig. 9a), and spessartine decreases from core to rim (Fig. 9b). Higher-grade garnets typically have subhedral, resorbed textures with significant zoning mainly near the rims. Pyrope is nearly constant in cores and decreases near rims and fractures (Fig. 9e). Spessartine is also nearly constant in garnet cores and generally increases near rims (Fig. 9f). Plagioclase is aligned in S_2 and typically unzoned, which we interpret to reflect the dynamic recrystallization of plagioclase during the development of S_2 and thus the composition that was present during the growth of the garnet rims.

Temperatures and pressures have been calculated for a preliminary suite of samples, some of which are summarized in Table 1 (M. L. Williams, unpublished data). The most important result of this work is illustrated in Figure 9 (c and f) and Table 2. Although temperatures vary significantly from amphibolite- to granulite-facies domains, pressures are ≈6 kbar along the entire canyon transect. The 6 kbar calculated pressures from the Upper Gorge are among the highest Paleoproterozoic metamorphic pressures reported in Arizona (cf. Alter et al., 1994). Most other terranes including the Transition Zone of central Arizona (Williams, 1991) and the Lower Granite Gorge of the Grand Canyon (Robinson, 1994) preserve pressures of 3–4 kbar. In the middle amphibolite–grade areas, most

TABLE 1. METAMORPHIC DOMAINS IN THE UPPER GRANITE GORGE, GRAND CANYON, ARIZONA

Red Canyon (Mile 77) to Vishnu Canyon (Mile 80) (upper amphibolite to granulite grade)
Sillimanite + biotite + garnet + plagioclase + quartz ± muscovite schists
Muscovite is generally coarse and poorly aligned and is interpreted to be retrograde. Where muscovite is locally fine grained and well foliated, it is probably prograde.
Migmatitic textures are common with boudinaged and folded pods and veins of granitic composition (leucosomes) and variably well-developed biotite selvages (melanosomes). Some components of the leucosome pods probably represent in situ or locally derived melts, but the dikelike geometries of other isolated leucosomes suggest that melt was also injected from deeper levels and dispersed during deformation.
Garnet shows evidence of resorption. Garnet and plagioclase commonly have overgrowths of more calcic plagioclase, interpreted to reflect late-stage decompression. Garnets show syn-S_2 inclusion-trail geometries where straight or broadly F_2-crenulated internal trails that sweep into the S_2 fabric orientation near garnet margins (see Fig. 10).
F_2 folding and shear-zone formation occurred during or after peak metamorphism, from the fact that F_2 folds deform sillimanite needles.
Calculated temperatures were on the order of 600–700 °C; pressures were ≈6 kbar.

Vishnu Fault, Mile 81
Mile 81 to Mile 85 (middle amphibolite grade)
Staurolite + garnet + biotite + muscovite + quartz + plagioclase schists
Peak metamorphism associated with F_2 shortening.
Rocks immediately west of the Vishnu fault (mile 80) contain late sillimanite, chlorite, and biotite, perhaps related to fluids or heating near the Vishnu fault.
Late andalusite near mile 84 indicates lower pressures (≈3 kbar) after 6 kbar metamorphism.
Mile 85 to Mile 96 (upper amphibolite to granulite grade)
Sillimanite + garnet + biotite + plagioclase + quartz pelitic rocks
Hornblende + plagioclase + garnet mafic rocks
Locally abundant pegmatite pods and granitic dikes.
Garnet + biotite and garnet + hornblende indicate temperatures of 650–725 °C and pressures of 6 kbar.
Local evidence for decompression during or after the metamorphic peak.

96-Mile Fault
Mile 96 to Mile 98 (upper greenschist to lower amphibolite grade)
Chlorite + muscovite + biotite + plagioclase + garnet + quartz + hornblende assemblages
No pegmatites exposed.
Calculated conditions near 500 °C and 6 kbar.
Minerals aligned in S_2; microstructures similar to higher-grade areas.

Crystal Shear Zone
Crystal Shear Zone (Mile 98) to Blacktail Canyon (Mile 119) (upper amphibolite grade)
Garnet + biotite + cordierite + plagioclase + quartz + muscovite schists
Orthoamphibole-bearing mafic rocks
Relict staurolite, typically with cordierite overgrowths, especially toward the east.
Garnet has texturally and compositionally distinct cores with sigmoidal inclusion trails and typical bell-shaped prograde zoning profiles; rims are subhedral with distinctly higher grossular contents and inclusion trails at a high angle to those in the cores.
Highest pegmatite density of any domain in the Upper Granite Gorge.
P-T determinations range widely depending on the compositions chosen for the calculations. Peak conditions interpreted to be 600–700 °C, but the mineral assemblages preserve a complex *P-T* history, perhaps reflecting pegmatite distribution and polyphase metamorphic history.

Note: Observations from this work and from Babcock (1990) and Clark (1976, 1979).

garnet cores overgrew the penetrative northwest-striking S_1 fabric (at 500–600 °C), while garnet rims that typically yield 6 kbar pressures overgrew different stages of the development of the S_2 cleavage (also at 500–600 °C; Fig. 9a). Many samples show compositional evidence for late-stage decompression, including low-Ca garnet overgrowths with high-Ca plagioclase inclusions and local late-stage andalusite in 6 kbar, sillimanite-bearing samples. On the basis of porphyroblast-matrix textures, and the presence of F_2 folds of an S_1 foliation defined by sillimanite, we infer that penetrative, northwest-striking, S_1 fabric development generally predated, but locally overlapped, the 6 kbar peak metamorphism and that the northeast-striking, subvertical fabric development took place during peak metamorphism and continued as the rocks were decompressed from 6 to 3 kbar.

Because peak pressures were relatively uniform throughout the transect, tectonic juxtaposition of different crustal levels cannot account for the temperature differences recorded across the transect. Instead, a major component of the temperature difference apparently resulted from advective heat transfer that elevated ambient temperatures of ≈500 °C by as much as 200 °C. A first-order observation (Campbell and Maxson, 1936; Babcock et al., 1974) is that the high-grade domains correlate with regions of high pegmatite density and that the relatively local variation in metamorphic grade may be attributed to regional metamorphism enhanced by heat provided by high metamorphic fluid flux and high pegmatite and/or granite dike densities in narrow (1–10 km wide) domains. Thus, we believe that the constant-*P* and variable-*T* character of the metamorphic domains reflects variable-temperature conditions, at least partially related to pegmatite density at ≈22 km deep in the crust during northwest-southeast directed shortening. The latter case is analogous to a model for pluton-enhanced metamorphism proposed for central Arizona (Williams, 1991), in which plutons may have elevated temperatures from a background temperature of 400–650 °C over 10s of kilometres adjacent to plutons. The general model is perhaps best illustrated between mile 77 and the Vishnu shear zone where calculated peak temperatures are between 650 and 725 °C and pegmatite dike densities are quite high. Immediately west of the Vishnu shear zone, peak temperatures are ≈500 °C, and pegmatite dike densities drop to zero within 300 m of the shear zone (Fig. 1). However, it is also likely that deformation associated with shear zones telescoped or truncated some of the pluton- or dike-related thermal gradients.

TECTONIC OVERVIEW

The Proterozoic evolution of the rocks exposed in the Granite Gorges of the Grand Canyon involves five principal stages (Fig. 10):

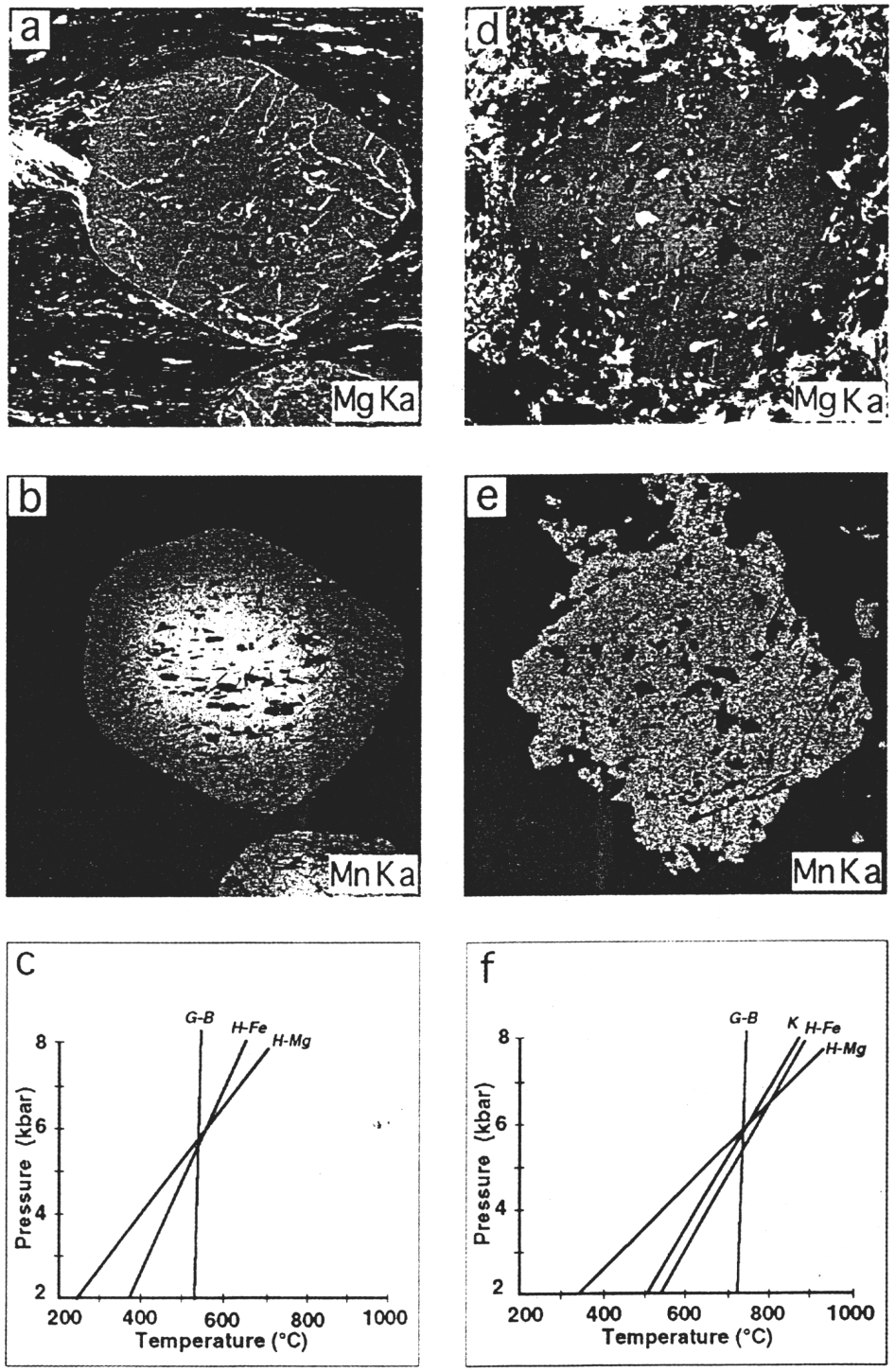

Figure 9. Comparison of amphibolite- and granulite-facies schists from the Upper Granite Gorge of the Grand Canyon. (a–c) Sample K3-83.8, from mile 83.8, contains staurolite, garnet, biotite, muscovite, chlorite, quartz, plagioclase, and ilmenite. (d–f) Sample K3-78.9, from mile 78.9, contains garnet, biotite, sillimanite, muscovite (retrograde?), quartz, and plagioclase. Note that garnet from the lower-grade sample is euhedral and exhibits prograde zoning. Garnet from the higher-grade sample is anhedral, and zoning, interpreted to reflect retrograde cooling and decompression, occurs mainly near the rim. Both garnet crystals are ≈5 mm in diameter. Calibrated thermobarometers for these assemblages yield consistent 6 kbar pressures, but temperatures vary by ≈200 °C. GB—garnet-biotite thermometer (Williams and Grambling, 1990). H-Fe, H-Mg—garnet-plagioclase-biotite-muscovite-quartz barometers (Hoisch, 1990) for Fe and Mg end-member reactions, respectively. K—garnet-plagioclase-sillimanite-quartz (GASP) barometer (Koziol and Newton, 1988). Compositions used for calculations are presented in Table 2.

TABLE 2: REPRESENTATIVE ELECTRON MICROPROBE ANALYSES FOR SAMPLES FROM FIGURE 9

Oxides	K3-78.9			K3-83.8					
(wt%)	Grt-core	Pl	Bt	Grt-core	Grt-rim	Bt	Ms	Chl	Pl
FeO	35.45	0.15	21.35	36.63	38.83	22.42	1.27	29.90	0.40
MgO	4.01	0.00	8.32	1.83	2.30	8.77	0.56	12.69	0.00
MnO	1.31	0.00	0.08	3.68	0.98	0.02	0.00	0.05	0.00
CaO	1.09	6.15	0.00	2.08	1.61	0.00	0.00	0.00	3.10
Na_2O	0.00	8.29	0.19	0.00	0.00	0.23	0.87	0.00	10.02
K_2O	0.00	0.07	9.17	0.00	0.00	8.21	9.31	0.00	0.09
TiO_2	0.02	0.00	2.43	0.00	0.00	1.53	0.23	0.09	0.00
Fe_2O_3	0.01	0.00	0.00	0.00	0.00	0.00	0.00	0.00	0.00
Al_2O_3	21.33	24.84	19.23	21.26	21.52	19.79	35.68	23.40	22.61
SiO_2	37.40	60.02	34.63	36.96	37.02	34.94	45.97	23.55	64.12
Total	100.62	99.52	95.4	102.436	102.26	95.91	93.89	89.68	100.34
	Number of oxygens								
Cations	12	8	11	12	12	11	11	11	8
Fe	2.365	0.006	2.742	2.448	2.589	2.855	0.142	2.641	0.015
Mg	0.477	0.000	1.904	0.218	0.273	1.991	0.112	1.998	0.000
Mn	0.089	0.000	0.010	0.249	0.066	0.003	0.000	0.004	0.000
Ca	0.093	0.295	0.000	0.178	0.138	0.000	0.000	0.000	0.146
Na	0.000	0.719	0.057	0.000	0.000	0.068	0.226	0.000	0.856
K	0.000	0.004	1.796	0.000	0.000	1.595	1.593	0.000	0.005
Ti	0.001	0.000	0.281	0.000	0.000	0.175	0.023	0.007	0.000
Fe	0.001	0.000	0.000	0.000	0.000	0.000	0.000	0.000	0.000
Al	2.005	1.310	3.480	2.002	2.022	3.552	5.640	2.913	1.174
Si	2.983	2.686	5.318	2.953	2.951	5.321	6.165	2.487	2.824

Note: Analyses made on a Cameca SX-50 electron microprobe at the University of Massachusetts.

(1) Early Stage, ca. 1.84 Ga. This stage, represented by the Elves Chasm pluton, involved the evolution of an intermediate-composition basement. The details of this stage are poorly known but are important in documenting basement fragments of Penokean age within the ca. 1.75 Ga arc terranes of the Southwest.

(2) Island-Arc Stage, 1.75–1.71 Ga. This stage (Fig. 10, a and b) involved (1) submarine bimodal volcanism that formed the Brahma and Rama Schists (1.75–1.74 Ga); (2) deposition of a thick section of generally immature sedimentary rocks (Vishnu Schist) such as graywacke, lithic arenites, and pelites in submarine arc-flanking basins; (3) emplacement of ca. 1.74–1.71 Ga arc plutons into the arc-related supracrustal rocks; and (4) early thrust-related deformation, presumably involving subduction and perhaps outboard collision of island arcs. The *P-T* path associated with this stage of tectonism probably involved heating to at least 400–500 °C and burial of rocks from 3 to 6 kbar due to crustal thickening by thrusting and isoclinal folding that produced a penetrative northwest-striking fabric. Future work on earlier accretionary stages should be directed to areas that record low peak-metamorphic temperatures, such as the 96-Mile Canyon to Crystal Creek domain, and to structures that might have an early accretionary history like the Crystal shear zone.

(3) Assembly Stage, 1.71–1.685 Ga. This stage (Fig. 10, c and d) involved complex modification of the arc-related rock packages during strong northwest-southeast shortening and partitioned middle-crustal flow. Magmatism during this stage was characterized by intrusion of granite plutons and associated dikes and dike networks. Deformation involved progressive, partitioned northwest-southeast shortening and subvertical extension that resulted in kilometre-wavelength folds of earlier penetrative tectonic layering and development of highly partitioned northeast-striking subvertical foliation. This segment of the *P-T* path is characterized by peak temperatures, strong (200 °C) lateral thermal gradients, and an interpreted clockwise-looping *P-T* path involving decompression from 6 to 3 kbar during crustal shortening (Fig. 9). Peak metamorphism, as well as the majority of strain associated with northwest-southeast shortening, took place between 1.70 and 1.685 Ga. Later stages (ca. 1.68–1.66 Ga) involved localized adjustments, an apparent rotation of the principal shortening axis, and accommodation features including retrograde movement of shear zones, kinks, and crenulation cleavages and development of mylonite fabrics in the cores of 1.685 Ga pegmatite dikes.

(4) Long-Term Mid-Crustal Residence at 3 kbar, 1.68–1.3 Ga. Local adjustments were probably followed by isobaric cooling of juvenile crust (Hodges et al., 1994) at 3 kbar. Evidence for long residence of this section of the crust at 3 kbar comes from studies of ca. 1.4 Ga plutons that show that regionally, these plutons intruded 3–4 kbar crustal levels (Anderson and Bender, 1989). Some 1.4 and post–1.4 Ga deformation has been documented by Nyman et al. (1994) in the Southwest, and this "event" may have affected the Grand Canyon region as movements on shear zones.

(5) Uplift and Erosion, 1.3–1.25 Ga. By ca. 1.3 Ga, crust in the region was uplifted to near sea level prior to deposition of the Grand Canyon Supergroup at ca. 1.3 Ga (Elston, 1989) and finally the eventual development of the Great Unconformity (Powell, 1876).

SUMMARY: INSIGHTS INTO MIDDLE-CRUSTAL PROCESSES

This section reviews evidence for the synchroneity and causal relationships among deformation, peak metamorphism at 6 kbar, and granitic plutonism at ca. 1.7 Ga and proposes a model for pluton-enhanced middle-crustal flow.

The transition from S_1 to S_2 deformation took place during peak metamorphism, as shown by microstructures. Garnet cores overgrew straight S_1 microstructures whereas garnet rims are syn-S_2. In domains recording high peak-metamorphic temperatures, sillimanite defines both S_1 and S_2. Finally, leucosomes (partial melts) are strongly deformed by S_1 and S_2 but also locally crosscut S_2 (Fig. 7). All these features show that peak metamorphism was synchronous with both S_1 and S_2.

F_2 deformation was also synchronous with granite plutonism. At mile 111, a 1697 Ma pegmatite exhibits nearly all F_2 shortening strain rel-

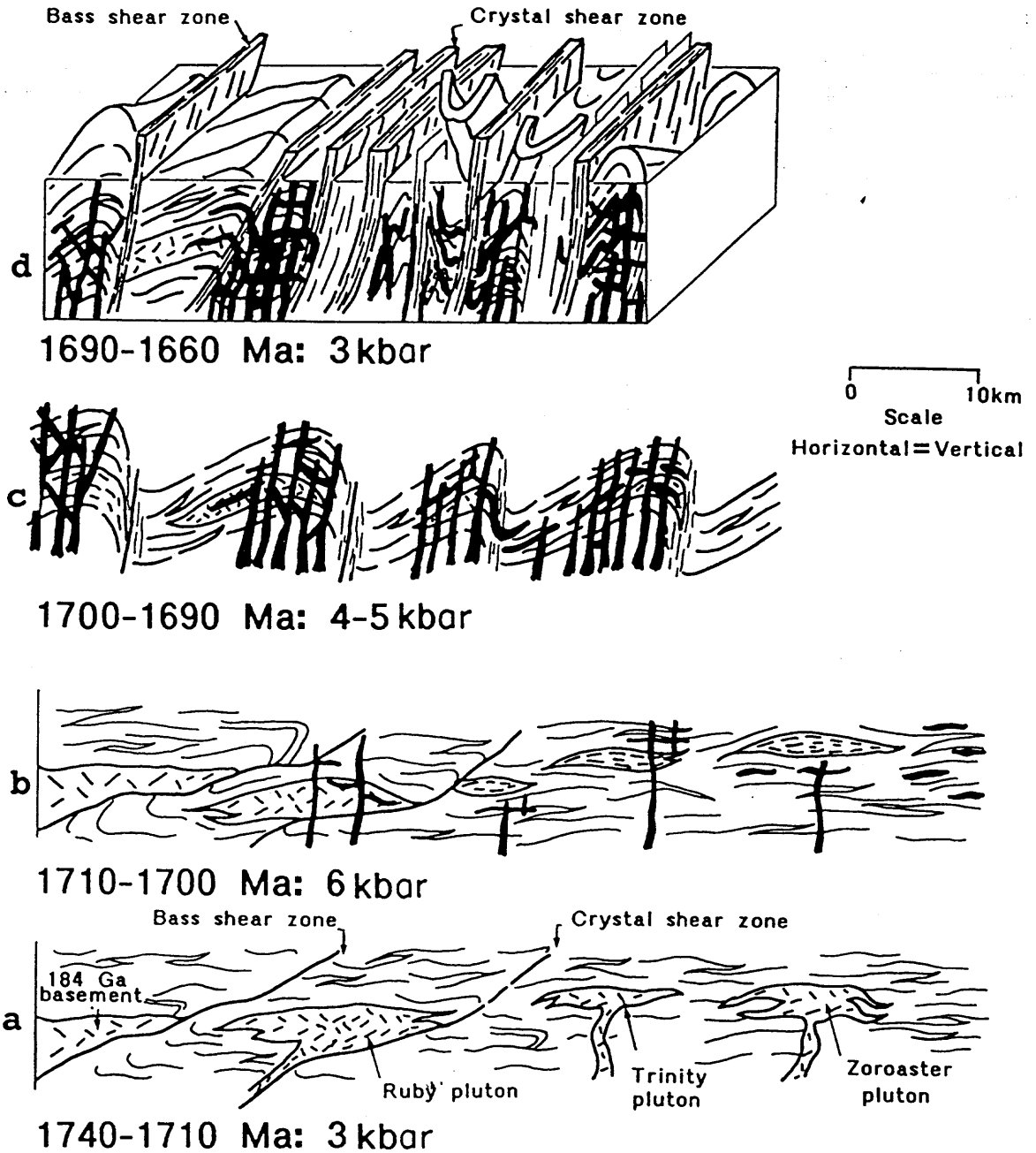

Figure 10. Schematic summary diagram for the Paleoproterozoic tectonic evolution of rocks exposed in the Upper Granite Gorge of the Grand Canyon. (a) 1.74–1.71 Ga. Arc-type plutons intruded supracrustal rocks at ≈3 kbar. Garnet cores, which record 3 kbar pressures, preserve northwest-striking fabrics. (b) 1.71–1.7 Ga. Rocks were compressed from 3 to 6 kbar, metamorphic monazites started growing by 1706 Ma, and crustal melting began at ca. 1.7 Ga. (c) 1.7–1.69 Ga. Shortening was northwest striking and southeast-northwest directed. The crust was decompressing; northwest-striking, variably dipping S_1 fabrics were being folded and transposed into northeast-striking vertical orientations; and magmas and metamorphic fluids were being focused into the hinge regions of incipient F_2 folds, enhancing moderately high ambient temperatures. (d) 1.69–1.66 Ga. Shortening was northwest striking and north-south directed. Decompression continued until the crust stabilized at ≈3 kbar; shear zones continued to accommodate minor adjustments; and granitic melts continued to intrude until ca. 1662 Ma (e.g., the Phantom pluton).

ative to folded S_1 in the area. In other areas, similar dikes are spectacularly folded by F_2 folds, whereas 1685 Ma dikes crosscut S_2 and are nearly undeformed by F_2 folding (Fig. 7). These dike geometries and timing relationships bracket F_2-S_2 strain to the interval 1700–1685 Ma and demonstrate that shortening and dike emplacement took place over a 15 m.y. progressive episode.

Peak metamorphism is related to granitic plutonism in time by the spatial association of dike networks with migmatitic regions recording the highest peak-metamorphic temperatures, on the basis of structural arguments (above) and overlapping monazite ages from schists and pegmatites. The latter suggest that monazite was growing or being reset over some interval during granitoid emplacement and northwest-southeast shortening.

Thus, our working hypothesis is that the orogenic history from 1.75 to 1.66 Ga can be viewed as a punctuated continuum of deformation, metamorphism, and magmatism, with a dominant pulse of granitic magmatism at 1.70–1.68 Ga synchronous with penetrative crustal shortening and peak metamorphism from 1.70 to 1.685 Ga. Island-arc lithologic sequences achieved 6 kbar pressures during thrust-related burial. The crust began heating such that metamorphic monazite grew by 1706 Ma and in situ melting formed migmatites beginning at ca. 1691 Ma. Peak shortening and metamorphism was accompanied by decompression to 3 kbar, suggesting that the combined shortening, heating, and magma emplacement instigated isostatic adjustments during orogeny.

We emphasize several constraints on any viable tectonothermal model for the history of Paleoproterozoic rocks exposed in the Upper Granite Gorge of the Grand Canyon. Observed metamorphic field gradients are spatially associated with pegmatite dike complexes, suggesting advective heat transport to the middle crust. Monazites in leucosomes from the mile 78 area have U-Pb ages (1706–1697 Ma) similar to monazites from crosscutting pegmatite dikes (1706–1692 Ma) (Hawkins et al., 1996) and are consistent with field relationships that show that crystallization of tabular granite dikes overlapped and outlasted peak metamorphism. Regional heating may have preceded dike emplacement, but the correlation of dike swarms with peak-metamorphic temperatures suggests pluton-enhanced metamorphism. Metamorphic mineral textures show peak metamorphism to have been synchronous with crustal shortening (S_2) and reactivation of S_1. Thus, textures temporally link metamorphism to deformation and indicate pervasive middle-crustal deformation. Also, deformed to undeformed dikes represent a continuum (even in one locality but especially over the region). The last observation indicates that granite plutonism was dominantly syndeformational. Thus, the mutual contemporaneity of plutonism, metamorphism, and deformation, plus the dramatic localization of heat, granitic intrusions, and F_2 deformation into localized zones, imply their mutual interaction.

ACKNOWLEDGMENTS

This work was partially supported by National Science Foundation grant EAR 920645 to Karlstrom and Williams. Ilg was supported by the Caswell Silver Fellowship from the University of New Mexico and two Geological Society of America grants. Glen Canyon Environmental Studies funded two river trips early in the study and provided high-resolution aerial photographs of the canyon corridor. The Grand Canyon National Park granted a research permit. Field work in the Grand Canyon was carried out as part of Ilg's M.S. thesis at Northern Arizona University and his Ph.D. thesis at the University of New Mexico. The manuscript benefited from thoughtful reviews by G. Haxel, S. Babcock, S. Reynolds, J. Selverstone, J. Geissman, and L. Walter.

REFERENCES CITED

Aerden, D. G. A. M., 1995, Porphyroblast non-rotation during crustal extension in the Variscan Lys-Caillaouas massif: Pyrenees: Journal of Structural Geology, v. 17, p. 709–725.

Alter, M. L., Reynolds, S. J., and Peacock, S. M., 1994, A high grade Proterozoic extensional shear zone in central Arizona: Geological Society of America Abstracts with Programs, v. 26, no. 7, p. A-231.

Anderson, C. A., and Silver, L. T., 1976, Yavapai Series—A greenstone belt, *in* Wilt, J. C., and Jenny, J. P., eds., Tectonic digest: Arizona Geological Society Digest, v. 10, p. 13–26.

Anderson, J. L., and Bender, E. E., 1989, Nature and origin of Proterozoic A-type granitic magmatism in the south-western United States of America: Lithos, v. 23, p. 19–52.

Babcock, R. S., 1990, Precambrian crystalline core, *in* Beus, S. S., and Morales, M., eds., Grand Canyon geology: New York, Oxford University Press, p. 11–28.

Babcock, R. S., Brown, E. H., and Clark, M. D., 1974, Geology of the older Precambrian rocks of the Upper Granite Gorge of the Grand Canyon, *in* Breed, W. S., ed., Geology of the Grand Canyon: Grand Canyon, Arizona, Grand Canyon Natural History Association, p. 2–10.

Babcock, R. S., Brown, E. H., Clark, M. D., and Livingston, D. E., 1979, Geology of the older Precambrian rocks of the Grand Canyon: Part II, The Zoroaster Plutonic Complex and related rocks: Precambrian Research, v. 8, p. 243–275.

Bennett, V. C., and DePaolo, D. J., 1987, Proterozoic crustal history of the western United States as determined by neodymium isotopic mapping: Geological Society of America Bulletin, v. 99, p. 674–685.

Bergh, S. C., and Karlstrom, K. E., 1992, The Chaparral shear zone: Deformation partitioning and heterogeneous bulk crustal shortening during Proterozoic orogeny in central Arizona: Geological Society of America Bulletin, v. 104, p. 329–345.

Billingsley, G. H., Jr., Breed, W. J., Sears, J. W., Ford, T. D., Clark, M. D., Babcock, R. S., and Brown, E. H., 1980, Geologic map of the eastern part of the Grand Canyon National Park: Grand Canyon, Arizona, Grand Canyon Natural History Association, scale 1:62 500.

Bowring, S. A., and Karlstrom, K. E., 1990, Growth and stabilization of Proterozoic lithosphere in the southwestern United States: Geology, v. 18, p. 1203–1206.

Brisbin, W. C., 1986, Mechanics of pegmatite intrusion: American Mineralogist, v. 71, p. 644–651.

Brown, E. H., Babcock, R. S., Clark, M. D., and Livingston, D. E., 1979, Geology of the older Precambrian rocks of the Grand Canyon: Part I, Petrology and structure of the Vishnu Complex: Precambrian Research, v. 8, p. 218–331.

Campbell, I., 1936, On the occurrence of sillimanite and staurolite in the Grand Canyon: Grand Canyon Natural History Bulletin, v. 5, p. 17–22.

Campbell, I., 1937, Types of pegmatites in the Archean at Grand Canyon, Arizona: American Mineralogist, v. 22, p. 436–445.

Campbell, I., and Maxson, J. H., 1933, Some observations on the Archean metamorphics of the Grand Canyon: U.S. National Academy of Science Proceedings, v. 19, p. 806–809.

Campbell, I., and Maxson, J. H., 1934, Geological studies of the Archean rocks at Grand Canyon: Carnegie Institution of Washington Year Book, v. 34, p. 323–326.

Campbell, I., and Maxson, J. H., 1935, Geological studies of the Archean rocks at Grand Canyon: Carnegie Institution of Washington Year Book, v. 35, p. 284–285.

Campbell, I., and Maxson, J. H., 1936, Geological studies of the Archean rocks at Grand Canyon: Carnegie Institution of Washington Year Book, v. 35, p. 329–331.

Campbell, I., and Maxson, J. H., 1937, Geological studies of the Archean rocks at Grand Canyon: Carnegie Institution of Washington Year Book, v. 36, p. 345–346.

Campbell, I., and Maxson, J. H., 1938, Geological studies of the Archean rocks at Grand Canyon: Carnegie Institution of Washington Year Book, v. 37, p. 359–364.

Clark, M. D., 1976, The geology and petrochemistry of the Precambrian metamorphic rocks of the Grand Canyon, Arizona [Ph.D. thesis]: Leicester, University of Leicester, 216 p.

Clark, M. D., 1979, Geology of the older Precambrian rocks of the Grand Canyon: Part III, Petrology of the mafic schists and amphibolites: Precambrian Research, v. 8, p. 277–302.

Condie, K. C., 1986, Geochemistry and tectonic setting of Early Proterozoic supracrustal rocks in the southwestern United States: Journal of Geology, v. 94, p. 845–864.

Darrach, M., Karlstrom, K. E., Argenbright, D. N., and Williams, M. L., 1991, Progressive deformation in the Early Proterozoic Shylock shear zone, Arizona: Arizona Geological Society Digest, v. 19, p. 97–116.

Davidson, C., Schmid, S. M., and Hollister, L. C., 1994, Role of melt during deformation in the deep crust: Terra Nova, v. 6, p. 133–142.

DePaolo, D. J., 1981, Neodymium isotopes in the Colorado Front Range and crust-mantle evolution in the Proterozoic: Nature, v. 271, p. 193–196.

Elston, D. P., 1989, Grand Canyon Supergroup, northern Arizona: Stratigraphic summary and preliminary paleomagnetic correlations with parts of other North American Proterozoic successions, *in* Jenney, J. P., and Reynolds, S. J., Geologic evolution of Arizona: Arizona Geological Society Digest, v. 17, p. 259–272.

Ford, T. D., Breed, W. J., and Mitchell, J. S., 1972, Name and age of Upper Precambrian basalts in the eastern Grand Canyon: Geological Society of America Bulletin, v. 83, p. 223–226.

Hawkins, D. P., Bowring, S. A., Ilg, B. R., Karlstrom, K. E., and Williams, M. L., 1996, U-Pb geochronologic constraints on Paleoproterozoic crustal evolution, Upper Granite Gorge, Grand Canyon, Arizona: Geological Society of America Bulletin (in press).

Henderson, J. B., Caldwell, W. G. E., and Harrison, J. E., 1980, North American Commission on Stratigraphic Nomenclature: Report 8, Amendment of code concerning terminology for igneous and high-grade metamorphic rock: Geological Society of America Bulletin, v. 91, p. 374–376.

Hobbs, B. E., Means, W. D., and Williams, P. F., 1976, An outline of structural geology: New York, John Wiley and Sons, 571 p.

Hodges, K. V., Hames, W. E., and Bowring, S. A., 1994, $^{40}Ar/^{39}Ar$ age gradients in micas from a high-temperature–low-pressure metamorphic terrane: Evidence for very slow cooling and implications for the interpretation of age spectra: Geology, v. 22, p. 55–58.

Hoffman, P. F., 1988, United plates of America, the birth of a craton: Early Proterozoic assembly and growth of Laurentia: Annual Review of Earth and Planetary Sciences, v. 16, p. 543–603.

Hoisch, T. D., 1990, Empirical calibration of six geobarometers for the mineral assemblage quartz + muscovite + plagioclase + garnet: Contributions to Mineralogy and Petrology, v. 104, p. 225–234.

Huntoon, P. W., Billingsley, G. H., Jr., Breed, W. J., Sears, J. W., Ford, T. D., Clark, M. D., Babcock, R. S., and Brown, E. H., 1980, Geologic map of the eastern part of the Grand Canyon National Park: Grand Canyon, Arizona, Grand Canyon Natural History Association, scale 1:62 500.

Ilg, B. R., 1992, Early Proterozoic structural geology of Upper Granite Gorge, Grand Canyon, Arizona [M.S. thesis]: Flagstaff, Northern Arizona University, 59 p.

Ilg, B. R., and Karlstrom, K. E., 1992, Early Proterozoic geology of Upper Granite Gorge, Grand Canyon, Arizona: Geological Society of America Abstracts with Programs, v. 24, no. 6, p. A-19.

Ilg, B. R., and Karlstrom, K. E., 1993, A transect of Early Proterozoic middle crust: Upper Granite Gorge, Grand Canyon, Arizona: Geological Society of America Abstracts with Programs, v. 25, no. 5, p. A-55.

Ilg, B. R., and Karlstrom, K. E., 1994, New 1:24,000 maps of Upper Granite Gorge, Grand Canyon, Arizona: Geological Society of America Abstracts with Programs, v. 26, no. 6, p. A-20.

Ilg, B. R., Karlstrom, K. E., Williams, M. L., and Hawkins, D. P., 1996, Older Precambrian geology of the eastern part of the Grand Canyon, *in* Huntoon, P. W., ed., Geology of the eastern part of the Grand Canyon: Grand Canyon, Arizona, Grand Canyon Natural History Association (in press).

Karlstrom, K. E., and Bowring, S. A., 1988, Early Proterozoic assembly of tectonostratigraphic terranes in southwestern North America: Journal of Geology, v. 96, p. 561–576.

Karlstrom, K. E., and Bowring, S. A., 1993, Proterozoic orogenic history in Arizona, Transcontinental Proterozoic provinces, chapter 4, *in* Van Schmus, W. R., and Bickford, M. E., eds., Precambrian of the conterminous U.S.: Boulder, Colorado, Geological Society of America, Geology of North America, v. C-2, p. 188–211.

Karlstrom, K. E., and Daniel, C. G., 1993, Restoration of Laramide right-lateral strike slip in northern New Mexico by using Proterozoic piercing points: Tectonic implications from the Proterozoic to the Cenozoic: Geology, v. 21, p. 1193–1142.

Koziol, A. M., and Newton, R. C., 1988, Redetermination of the garnet breakdown reaction and improvement of the plagioclase-garnet-Al_2SiO_5-quartz geobarometer: American Mineralogist, v. 73, p. 216–223.

Lingley, W. S., 1973, Geology of the older Precambrian rocks in the vicinity of Clear Creek and Zoroaster Canyon, Grand Canyon, Arizona [M.S. thesis], Bellingham, Western Washington University, 78 p.

Livingston, D. E., Brown, E. H., Babcock, R. S., and Clark, M. D., 1974, Rb-Sr whole rock isochrons for "older" Precambrian plutonic and metamorphic rocks of the Grand Canyon, Arizona: Geological Society of America Abstracts with Programs, v. 6, p. 848–849.

Lucchitta, I., and Beus, S. S., 1987, Field trip guide for Marble Canyon and eastern Grand Canyon, *in* Davis, G. H., and VandenDolder, E. M., eds., Geological diversity of Arizona and its margins: Excursions to choice areas: Arizona Bureau of Geology and Mineral Technology Special Paper 5, p. 3–19.

Maxson, J. H., 1968, Geologic map of the Bright Angel quadrangle, Grand Canyon National Park, Arizona (revised): Grand Canyon, Arizona, Grand Canyon Natural History Association, scale 1:48 000.
Naeser, C. W., Duddy, I. R., Elston, D. P., Dumitru, T. A., and Green, P. F., 1989, Fission-track dating: Ages for Cambrian strata, and Laramide and post–middle Eocene cooling from the Grand Canyon, Arizona, *in* Elston, D. P., Billingsley, G. H., and Young, R. A., Geology of Grand Canyon, northern Arizona (with Colorado River guides): American Geophysical Union, Field Trip Guidebook T115/315, p. 139–144.
Noble, L. F., and Hunter, J. F., 1916, Reconnaissance of the Archean Complex of the Granite Gorge, Grand Canyon, Arizona: U.S. Geological Survey Professional Paper 98–I, p. 95–113.
Nyman, M. W., Karlstrom, K. E., Kirby, E., and Graubard, C. M., 1994, Mesoproterozoic contractional orogeny in western North America: Evidence from ca. 1.4 Ga plutons: Geology, v. 22, p. 901–904.
Pasteels, P., and Silver, L. T., 1965, Geochronological investigations in the crystalline rocks of the Grand Canyon, Arizona: Geological Society of America Abstracts with Programs, p. 122.
Powell, J. W., 1876, Exploration of the Colorado River of the West: Washington, D.C., Smithsonian Institution, 291 p.
Ragan, D. M., and Sheridan, M. F., 1970, The Archean rocks of the Grand Canyon, Arizona: Geological Society of America Abstracts with Programs, v 2, no. 2, p. 132–133.
Robinson, K., 1994, Metamorphic petrology of the Lower Granite Gorge and the significance of the Gneiss Canyon shear zone, Grand Canyon, Arizona [M.S. thesis]: Amherst, University of Massachusetts, 187 p.
Sears, J. W., 1973, Structural geology of the Precambrian Grand Canyon Series [M.S. thesis], Laramie, University of Wyoming, 100 p.
Shoemaker, E. M., Squires, R. L., and Abrams, M. J., 1978, Bright Angel and Mesa Butte fault systems of northern Arizona, *in* Smith, R. B., and Eaton, G. P., eds., Cenozoic tectonics and regional geophysics of the western Wordillera: Geological Society of America Memoir 152, p. 341–367.
Vallance, T. G., 1967, Mafic rock alteration and isochemical development of some cordierite-anthophyllite rocks: Journal of Petrology, v. 8, p. 84–96.
Van Schmus, W. R., and 24 others, 1993, Transcontinental Proterozoic provinces, *in* Reed, J. C., Jr., et al., eds., Precambrian: Conterminous U.S.: Boulder, Colorado, Geological Society of America, Geology of North America, v. C-2.
Walcott, C. D., 1890, Study of a line of displacement in the Grand Canyon of the Colorado in northern Arizona: Geological Society of America, v. 1, p. 49–64.
Walcott, C. D., 1894, Precambrian igneous rocks of the Unkar Terrane, Grand Canyon of the Colorado: U.S. Geological Survey 14th Annual Report for 1892/93, Part 2, p. 497–519.
Walcott, C. D., 1895, Algonkian rocks of the Grand Canyon: Journal of Geology, v. 3, p. 312–330.
Walen, M. B., 1973, Petrogenesis of the granitic rocks of part of the Upper Granite Gorge, Grand Canyon, Arizona [M.S. thesis]: Bellingham, Western Washington University, 92 p.
Williams, M. L., 1991, Overview of Proterozoic metamorphism in Arizona, *in* Karlstrom, K. E., ed., Proterozoic geology and ore deposits of Arizona: Arizona Geological Society Digest, v. 19, p. 11–26.
Williams, M. L., and Grambling, J. A., 1990, Manganese, ferric iron, and the equilibrium between garnet and biotite: American Mineralogist, v. 75, p. 886–908.
Williams, P. F., 1985, Multiply deformed terrains—Problems of correlation: Journal of Structural Geology., v. 7, p. 269–280.
Williams, P. F., and Zwart, H. J., 1977, A model for the development of the Seve-Koli Caledonian nappe complex, *in* Saxena, S., and Bhattacharji, eds., Energetics of geological processes: New York, Springer-Verlag, p. 170–187.
Wooden, J. L., and DeWitt, E., 1991, Pb evidence for a major crustal boundary in western Arizona, *in* Karlstrom, K. E., ed., Proterozoic geology and ore deposits of Arizona: Arizona Geological Society Digest, v. 19, p. 27–50.

MANUSCRIPT RECEIVED BY THE SOCIETY MARCH 24, 1995
REVISED MANUSCRIPT RECEIVED JANUARY 17, 1996
MANUSCRIPT ACCEPTED FEBRUARY 16, 1996

Printed in U.S.A.

GEOLOGICAL SOCIETY OF AMERICA

BULLETIN

ISSN 0016-7606 VOLUME 108 NUMBER 9 SEPTEMBER 1996

In this issue:

Carbonate content of [illegible] and geomorphology

Kinematic models for [illegible] and mantle exhumation

Transient stress [illegible] of a thrust she[illegible]

GEOLOGICAL SOCIETY OF AMERICA
BULLETIN
VOLUME 108, NUMBER 9, SEPTEMBER 1996

CONTENTS

ON THE COVER

Computer-enhanced, color composite rendition of Landsat Thematic Mapper image recorded over the central Amazon River, August 10, 1991. The annual flood has receded ≈2 m, the floodplain is draining, and flow is from left to right (west to east). The color of the main channel indicates relatively high sediment concentrations in the water. The main channel is ≈3–4 km across. See "Channel-floodplain geomorphology along the Solimões-Amazon River, Brazil" by Leal A. K. Mertes, Thomas Dunne, and Luiz A. Martinelli. Image provided by E. Novo and T. Krug, INPE—Brazil.

Authors of manuscripts submitted for the *Bulletin* should mail four complete copies to *Bulletin*, Geological Society of America, P.O. Box 9140, Boulder, CO 80301. Authors should follow the guidelines published in the *Bulletin* (part 1, text and figures, August 1996, v. 108. p. 1068–1072; part 2, tables, September 1996, v. 108, p. 1197–1198). Copies of these are also available by mail from the *Bulletin* Editorial Office in Boulder. Authors should retain originals of illustrations until these are requested. The author must state in a cover letter that the paper has not been previously published and is not and will not be submitted for publication elsewhere while it is in review for the *Bulletin*.

GSA requests voluntary page charge contributions of $125 per page for *Bulletin* articles. The acceptance of a manuscript for publication is not contingent upon the payment of contributions.